



1 **Root water uptake patterns are controlled by tree species** 2 **interactions and soil water variability**

3 Gökben Demir¹, Andrew J. Guswa², Janett Filipzik¹, Johanna Clara Metzger^{1,3}, Christine Römermann^{4,6},
4 Anke Hildebrandt^{1,5,6}

5 ¹ Group of Terrestrial Ecohydrology, Institute of Geoscience, Friedrich Schiller University Jena, Jena,
6 07749, Germany

7 ² Picker Engineering Program, Smith College, Northampton, MA, 01063, USA

8 ³Institute of Soil Science, University of Hamburg, Hamburg, 20146, Germany

9 ⁴Plant Biodiversity, Institute of Ecology and Evolution, Friedrich Schiller University Jena, Jena, 07743,
10 Germany

11 ⁵ Department of Computational Hydrosystems, Helmholtz Centre for Environmental Research – UFZ,
12 Leipzig, 04318, Germany

13 ⁶German Centre for Integrative Biodiversity Research (iDiv) Halle -Jena-Leipzig, Leipzig, 04103,
14 Germany

15

16 Correspondence to: goekben.demir@uni-jena.de and anke.hildebrandt@ufz.de

17 **Abstract**

18 Throughfall is the largest source of water entering the soil in forests, and its spatial distribution depends
19 on several biotic and abiotic factors. It is well documented that the distribution of throughfall results in
20 reoccurring higher and lower water inputs at certain locations. However, the role of horizontal root water
21 uptake patterns in understanding the effects of throughfall patterns on subsurface water dynamics remains
22 unresolved. Therefore, here we investigate root water uptake patterns by considering spatial patterns of
23 throughfall and soil water patterns in addition to soil and neighboring tree characteristics. In a beech-
24 dominated mixed deciduous forest in a temperate climate, we conducted weekly intensive throughfall
25 sampling at locations paired with soil moisture sensors during the 2019 growing season. We employed a
26 linear mixed effects model to understand controlling factors for root water uptake patterns. Our results
27 show that soil water patterns and interactions among neighbouring trees are the most significant factors
28 regulating root water uptake patterns. Temporally stable throughfall patterns did not influence root water
29 uptake patterns. Similarly, soil properties were unimportant for spatial patterns of root water uptake. We



30 found that wetter locations (rarely associated with throughfall hotspots) promoted greater root water
31 uptake. Root water uptake in monitored soil layers also increased with neighbourhood species richness.
32 Ultimately our findings suggest that complementarity mechanisms within the forest stand, in addition to
33 soil water variability and availability, govern root water uptake patterns.

34

35 **Key words:** root water uptake, throughfall, soil water, spatial patterns, beech

36 1) Introduction

37 Vegetation intercepts and redirects precipitation into throughfall and stemflow, collectively referred to as
38 below-canopy precipitation. Moreover, throughfall is usually the largest component of below canopy
39 precipitation (Levia and Frost, 2006; Sadeghi et al., 2020). For instance, in temperate forests throughfall
40 can account for about 70% of above canopy precipitation (Levia and Frost, 2003; Sadeghi et al., 2020).
41 This makes it the primary source of soil moisture replenishment in vegetated areas.

42 Below-canopy precipitation is modified by several biotic and abiotic factors (Levia and Frost, 2006; Levia
43 et al., 2011), such as vegetation type and canopy architecture (Crockford and Richardson, 2000; Pypker
44 et al., 2011; Levia et al., 2017), forest structure (Rodrigues et al., 2022), meteorological elements such as
45 wind speed (Staelens et al., 2008; Van Stan et al., 2011; Fan et al., 2015), precipitation intensity and event
46 size (Dunkerley, 2014; Magliano et al., 2019; Zhang et al., 2016; Staelens et al., 2008). This implies that
47 it inherently varies across space and time. Furthermore, previous studies showed that the spatial
48 distribution of throughfall persists repeatedly over time (Keim et al., 2005; Staelens et al., 2006; Guswa
49 and Spence, 2012; Carlyle-Moses et al., 2014; Metzger et al., 2017; Van Stan et al., 2020).

50 Throughfall patterns potentially translate their spatial variability into soil moisture (Raat et al., 2002;
51 Blume et al., 2009; Zimmermann et al., 2009; Zehe et al., 2010; Bachmair et al., 2012; Rosenbaum et al.,
52 2012; Zhang et al., 2016). A decade ago Coenders-Gerrits et al., (2013) proposed that throughfall patterns
53 are translated into soil wetting dynamics with a model based on combined hillslope topographic and
54 throughfall data collected in a beech-dominated catchment. However, in this model, the effect of
55 throughfall patterns on soil moisture patterns rapidly ceased. Later, Metzger et al. (2017) empirically



56 confirmed that throughfall patterns barely alter soil moisture in response to rainfall and the limited
57 influence rapidly disappears. Recently, Zhu et al. (2021) observed that stable spatial patterns of
58 throughfall were related to the spatial distribution of soil moisture. However, this relationship was
59 restricted only to relatively wet soil locations and throughfall hotspots. They also showed that throughfall
60 patterns had a weak influence on the temporal dynamics of soil water content compared to soil bulk
61 density and litter layer properties.

62 Previously proposed explanations for the weak and short-term influence of throughfall patterns on the
63 soil moisture patterns include: soil properties (Metzger et al., 2017), preferential flow induced by dry
64 antecedent soil conditions (Jost et al., 2004; Blume et al., 2009; Molina et al., 2019; Fischer et al., 2023),
65 litter layer (Raat et al., 2002), and local root water uptake enhanced by throughfall hotspots (Bouten et
66 al., 1992; Coenders-Gerrits et al., 2013). Based on a one-dimensional soil water model, Bouten et al.
67 (1992) proposed that throughfall patterns alter and localize root water uptake and promote fast drainage
68 via preferential flow paths. However, to the best of our knowledge, the feedback mechanism of
69 throughfall patterns on root water uptake variation has not yet been investigated in the field. Therefore, it
70 is unclear how water uptake patterns play a role in translating throughfall patterns into spatio-temporal
71 variation of soil water and vice versa.

72 Soil water distribution may shape root water uptake patterns even more than root networks (Kühnhammer
73 et al., 2020). Soil properties control soil water redistribution (Grayson et al., 1997; Cosh et al., 2008;
74 Jarecke et al., 2021) and water availability (Vereecken et al., 2007; Cai et al., 2018). Thus soil properties
75 can influence root water uptake patterns (Nadezhdina et al., 2007; Kirchen et al., 2017). Moreover,
76 variations in soil water content reflect water uptake by root systems (Hupet et al., 2002; Schume et al.,
77 2004; Schwärzel et al., 2009; Guderle and Hildebrandt, 2015; Jackisch et al., 2020). On the flip side, root
78 water uptake can amplify but mostly homogenize soil moisture distribution (Hupet and Vanclooster,
79 2005; Teuling and Troch, 2005; Ivanov et al., 2010; Baroni et al., 2013; Martínez García et al., 2014).
80 Root networks can also regulate soil moisture distribution by transporting water from wetter places to
81 drier locations, which has been observed in a variety of ecosystems (e.g., Emerman and Dawson, 1996;
82 Katul and Siqueira, 2010; Yu and D'Odorico, 2015; Priyadarshini et al., 2016; Hafner et al., 2017).



83 In addition, tree species richness affects the dynamics of root water uptake (e.g., Volkman et al., 2016;
84 Spanner et al., 2022). Neighboring different tree species utilize different hydraulic strategies, such as
85 extracting water from different soil depths (Silvertown et al., 2015; Guo et al., 2018; Brum et al., 2019).
86 However, soil water scarcity can initiate or enhance competition mechanisms for water among tree species
87 (González de Andrés et al., 2018; Vitali et al., 2018; Magh et al., 2020). Moreover, studies conducted in
88 temperate forest ecosystems demonstrate that the relationship between tree species richness and water
89 uptake mechanisms varies (Krämer and Hölscher, 2010; Kunert et al., 2012; Meißner et al., 2012;
90 Forrester, 2014; Lübbe et al., 2016).

91 Briefly, throughfall and soil water variability, soil properties, and root water uptake patterns form complex
92 and intertwined interactions in the terrestrial hydrological cycle. It has not yet been shown empirically
93 how root water uptake patterns are affected by throughfall and soil water variation in combination with
94 soil properties and neighboring tree characteristics. Therefore, here we investigate the role of throughfall
95 patterns and pose the following questions to guide the investigation:

- 96 i) How do throughfall patterns influence root water uptake patterns?
- 97 ii) How do soil water and its variation and soil properties control variation in root water uptake?
- 98 iii) What is the role of biotic factors, namely tree size, distance, number, and species richness, on
99 root water uptake patterns?

100 Here, we address these questions by employing linear mixed effects model based on weekly throughfall
101 sampling at locations paired with intensive soil moisture measurements in a beech-dominated unmanaged
102 forest. In addition, we incorporate data on field capacity, bulk density, and neighboring tree
103 characteristics.

104 **2) Materials and Methods**

105 **2.1) Research Site and Field Sampling**

106 **2.1.1) Research Site**

107 The research site is located in the forested upper hill region of the Hainich low mountain range in
108 Thuringia, Germany, as a part of the Hainich Critical Zone Exploratory (CZE) (Küsel et al., 2016). The



109 altitude in the research site ranges from 362 m to 368 m a.s.l. Mean annual air temperature varies between
110 7.5 and 9.5 °C, and the mean annual precipitation ranges from less than 600 to 1000 mm in the CZE
111 (Küsel et al., 2016).

112 In the study area, thin-bedded alternations of limestones and marlstones of carbonate rock (Middle
113 Triassic) form the bedrock overlain by shallow Pleistocene loess layer with cambisols and luvisols as
114 dominant soil types (IUSS Working Group, 2006; Metzger et al., 2021). The median soil depth above the
115 weathered bedrock is 37 cm, with soil depths ranging from 15 cm to a maximum depth of 87 cm (Metzger
116 et al., 2017).

117 In 2019, the tree community in the research site consisted of 574 individuals of various ages (diameter at
118 breast height \geq 5cm). The dominant species is European beech (*Fagus sylvatica* L.), which makes up 70%
119 of the tree community, followed by sycamore maple (*Acer pseudoplatanus* L.) with 21 %, and European
120 ash (*Fraxinus excelsior* L.) with 4%. These dominant species are accompanied by Large-leaved linden
121 (*Tilia platyphyllos* Scop.), European hornbeam (*Carpinus betulus* L.), Norway maple (*Acer platanoides*
122 L.), Scots elm (*Ulmus glabra* L.), and Wild service tree (*Sorbus torminalis* (L.) Crantz). The stand has a
123 total basal area of 40 m² ha⁻¹ and has been unmanaged since 1997 (Kohlhepp et al., 2017).

124 **2.1.2) Soil moisture monitoring and soil properties**

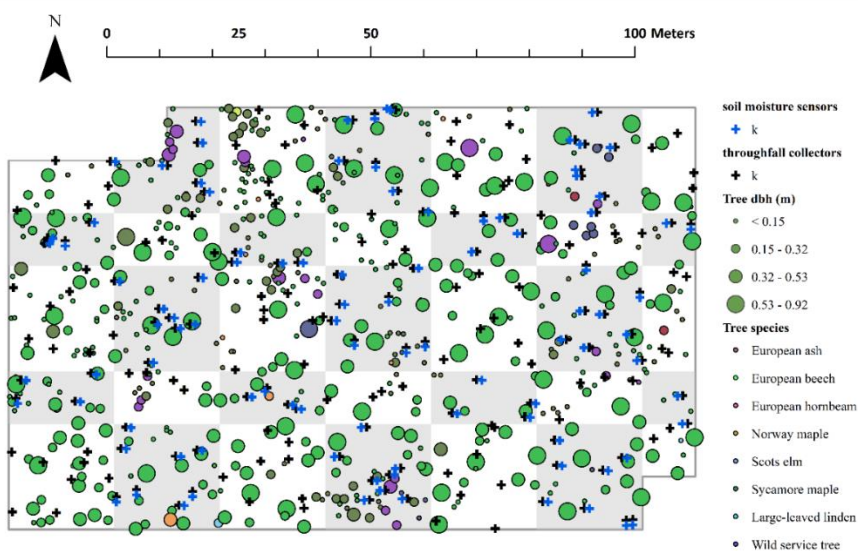
125 The forest site (1 ha) was equipped with a soil moisture monitoring network (SoilNet; Bogen et al., 2010)
126 consisting of SMT100 frequency domain sensors (Treuebner GmbH, Neustadt, Germany). Metzger et al.
127 (2017) first described the soil moisture monitoring setup. Briefly, the observation platform (Figure 1) was
128 divided into 100 subplots (10 m \times 10 m), and 49 subplots were equipped with soil moisture sensors at
129 two random measuring points each, for a total of 98 locations. At each measuring point, sensors were
130 placed at two different depths, 7.5 cm (top sensors) and 27.5 cm (bottom sensors). The soil moisture
131 network is maintained through a regular bi-weekly routine to avoid potential failures such as depleted
132 sensors batteries, hardware problems, etc.

133 Undisturbed soil samples were collected during the sensor installation in 2014 and 2015 to estimate bulk
134 density and water content at field capacity. In addition, we collected additional disturbed soil samples (n
135 = 40) near sensor locations in 2019. Bulk density was determined from oven-dried (24h, 105°C) soil mass



136 weight and water content at field capacity by applying 60 hPa pressure to the saturated undisturbed sample
137 for 72 h.

138 Soil properties vary slightly from top to subsoil at the research site. While silty loam is the dominant soil
139 texture in both layers, the clay content is higher in the subsoil (Metzger et al., 2021). The median
140 volumetric water content at the field capacity is 44% in the topsoil and 42% in the subsoil. Moreover, the
141 water content at the field capacity varies from 27% to 60% and from 31% to 62% in the topsoil and
142 subsoil, respectively. The average bulk density (d_{bulk}) of the topsoil is 1.16 g cm^{-3} , with a range of 0.73 to
143 1.5 g cm^{-3} . In the subsoil, the average bulk density (d_{bulk}) is slightly higher at 1.37 g cm^{-3} but has a similar
144 range ($0.7 - 1.6 \text{ g cm}^{-3}$) (See supplement for details).



145

146 **Figure 1** (above) The photo of the site. (below) the field monitoring setup of stratified randomly distributed throughfall
147 collectors and soil moisture sensors together with the trees which are sized according to the diameter at breast height (dbh)
148 and coloured according to the species. Throughfall collectors are paired with soil moisture sensors at 98 locations (n=182) in
149 the grey shaded subplots. White coloured subplots are equipped with only throughfall collectors.



150 **2.1.3) Gross precipitation and throughfall sampling**

151 Five gross precipitation funnels were placed 1.5 m above ground level in an adjacent open grassland (ca.
152 250 m distance to the research site). As described in Metzger et al. (2017) and Demir et al. (2022), the
153 precipitation funnels were made of a circular plastic funnel (12 cm in diameter) and sampling bottle (2 L
154 in volume), and ping pong balls were placed in the funnel orifice to prevent evaporation losses.

155 During the early growing season of 2019, we placed throughfall collectors in soil moisture monitoring
156 subplots at 98 locations. We paired these throughfall collectors with the soil moisture sensors by placing
157 them within 1 m of each other. The paired collectors were placed down-slope to avoid interference with
158 soil moisture measurements. For the rest of the research site, in 51 other subplots, we adopted a separate
159 independent stratified random design from Metzger et al. (2017). Briefly, we placed two throughfall
160 collectors in each subplot that was not equipped with soil moisture sensors. All throughfall collectors
161 were placed roughly 37 cm above the ground.

162 We conducted weekly manual measurement of throughfall and gross precipitation during the 2019
163 growing season (April to August). We measured gross precipitation and throughfall on rainless days
164 therefore, in some of the sampling weeks, the interval between field measurements ranged between six
165 and eight days.

166 We used the paired throughfall collectors ($n = 98$) to identify the drivers of root water uptake patterns as
167 we derived root water uptake values based on soil water content measurements (see below). However, we
168 used all randomly placed throughfall collectors ($n = 200$) to describe the spatio-temporal variation of
169 throughfall within the research site.

170 **2.2) Estimation of potential evapotranspiration**

171 We calculated the daily potential evapotranspiration by applying the concept of thermodynamic limits of
172 convection (Kleidon and Renner, 2013):

$$173 E_{\text{pot}} = \frac{1}{\lambda} \frac{s}{s + \gamma} \frac{R_{\text{sn}}}{2} \quad (1)$$

174 Where R_{sn} is absorbed solar radiation (W m^{-2}), λ is the latent heat of vaporization, γ is the psychrometric
175 constant, and s is the slope of the saturation vapor pressure curve.



176 Here, we acquired solar radiation, air temperature, and precipitation data for the throughfall sampling
177 period from a nearby weather station ("Reckenbuel") which is located approximately 1.4 km northeast of
178 the research site and provides data in 10 minutes intervals. The site-specific albedo for the summer period
179 was adopted from Otto et al. (2014).

180 In addition, we used the precipitation data measured at the weather station to define rain events and dry
181 periods, as described below.

182 **2.3) Data analysis**

183 **2.3.1) Quality control of soil water content data**

184 We systematically reviewed the six-minute soil water content data for quality control in two steps: 1)
185 identification of problems (such as jumps to extremely low and high values, duplicated time stamps of
186 different values, long discontinuities in the measurements, and lack of temporal variation in the time series
187 despite rain events), 2) classification and removal of detected outliers and irregularities. We visually
188 identified and removed unrealistic measurements such as extremely low (< 5 vol-%) and high values far
189 beyond the field capacity (> 75 vol-%) and long plateaus of repeated values despite rain events. We also
190 excluded the time series that exhibited long-term discontinuities that prevented us from calculating root
191 water uptake. During the visual inspection, we eliminated values with duplicated time stamps that violated
192 the actual temporal trend. Next, we scanned the data using the Hampel filter function of the 'pracma' R
193 package (Borchers, 2021) with customized moving window length and Pearson's rule threshold value
194 (Pearson, 1999) to flag possible outliers.

195 Despite regular maintenance, many sensors failed to meet the quality criteria in the growing season
196 (March-August) in 2019. Only 56 sensor locations (out of 98) simultaneously provided high-quality data
197 from both top and bottom sensors with different time intervals throughout the season. Of these, only 34
198 sensor locations provided data for the root water uptake estimation.

199 **2.3.2) Soil water calculation**

200 We estimated soil water (S) at measurement locations for the monitored soil layer based on volumetric
201 soil water content measured by top and bottom sensors.



202 $S_{i,d} = \sum z_t \theta_{i,d}^t + z_b \theta_{i,d}^b$ (2)

203 We similarly integrated the soil water at field capacity ($S_{FC,i}$),

204 $S_{FC,i} = \sum z_t \theta_{FC,i}^t + z_b \theta_{FC,i}^b$ (3)

205 where z_t is the depth of the soil column monitored by the top sensor and z_b is the depth of soil represented
206 by the bottom sensor, and $\theta_{i,d}$ is a volumetric soil water content at location i on date d , and $\theta_{FC,i}$ the soil
207 water content at the field capacity.

208 We calculated bulk density at the sensors' locations for the monitored soil layer.

209 $d_{bulk,i} = \frac{\sum z_t d_{bulk,i}^t + z_b d_{bulk,i}^b}{\sum z_t + z_b}$ (4)

210 where $d_{bulk,i}^t$ and $d_{bulk,i}^b$ are the bulk density of the topsoil and subsoil, respectively, at location i .

211 2.3.3 Descriptive Statistics

212 We calculated the coefficient of quartile variation (CQV) and the interquartile range to describe spatial
213 variation of throughfall, volumetric soil water content, and root water uptake. Also, we estimated octile
214 skewness (OS_8) of throughfall based on the first and seventh octile and standard deviation (SD) of the
215 estimated daily root water uptake.

216 $CQV = \frac{Q_3 - Q_1}{Q_3 + Q_1}$ (5)

217 $OS_8 = \frac{(Q_7 - median) - (median - Q_1)}{Q_7 - Q_1}$ (6)

218 We characterized spatial patterns of daily root water uptake (E_t) by calculating the spatial deviation from
219 the mean ($\delta E_{t,i,d}$, Equation 7) (Vachaud et al., 1985).

220 $\delta E_{t,i,d} = \frac{E_{t,i,d} - \overline{E_{t,d}}}{\overline{E_{t,d}}}$ (7)

221 where $E_{t,i,d}$ is daily root water uptake estimated at i sensor location on date d and $\overline{E_{t,d}}$ is spatial average
222 of daily root water uptake on date d .

223 Similarly, we calculated the spatial deviation of soil water and throughfall to identify their spatial patterns.



224 2.4) Root water uptake estimation

225 We estimated root water uptake using the multi-step, multi-layer regression method (MSML), which
226 derives evapotranspiration from diurnal differences in soil water content (Guderle and Hildebrandt, 2015;
227 Guderle et al., 2018). This approach does not require prior information on root structure but relies on high
228 temporal and spatial resolution data on multiple soil layers.

229 As described in Guderle and Hildebrandt (2015), the MSML derives root water uptake from distinct
230 differences in the day and night portions of soil moisture time series. The main assumption is that in the
231 absence of rainfall-driven rapid vertical soil water flow, evapotranspiration occurs only during the day,
232 while soil water flow occurs both during the day and at night. As a result, soil moisture time series reflect
233 a distinct day/night signal under dry weather conditions. This method has previously been applied to
234 estimate transpiration in both forest and grassland ecosystems (Guderle et al., 2018; Jackisch et al., 2020).
235 Therefore, we first excluded potential periods of fast vertical flow periods from the time series due to
236 previous rainfall events and identified periods for estimating daily root water uptake. We considered 8 h
237 buffer period to include canopy dripping and 48 h for the cessation of rainfall influence on soil water.
238 Thus, a total of 56 h was the time interval used to define the water uptake estimation period. The period
239 when the root water uptake is estimated is hereafter referred to as the dry period.

240 Next, we split each soil moisture time series into a day (transpiration active period) and a night branch,
241 as Guderle and Hildebrandt (2015) explained. We defined the transpiration period (starts 2 h after sunrise
242 and ends 2 h before sunset) based on local sunrise and sunset time. Sunrise and sunset times were obtained
243 from the R package 'suncal' (Thieurmél and Elmarhraoui, 2022). We fit linear models to each split branch
244 of the time series and derived the slopes. The difference between the slope of the day branch (m_{tot}) and
245 the average slope of the antecedent and preceding night ($\overline{m_{flow,t}}$) gives the rate of water uptake. Thus, we
246 estimated daily evapotranspiration at each soil water content location i (Equation 8, 9) by accounting for
247 soil layer thickness and slope difference.

248

$$249 E_{t,msml,i}^{t,b} = (m_{tot,i}^{t,b} - \overline{m_{flow,t}^{t,b}}) d_{z,i}^{t,b} \quad (8)$$

$$250 E_{t,i} = \sum(E_{t,msml,i}^t + E_{t,msml,i}^b) \quad (9)$$



251

252 **2.5) Linear Mixed Effects Model**

253 We employed a linear mixed effects model to investigate the driving factors for root water uptake patterns.

254 A linear mixed effects model is a multivariate statistical tool. It describes the relationship between a
255 dependent variable and explanatory variables (fixed effects) while controlling for dependencies in the
256 data that may arise due to repeated sampling with certain designs (random effects).

257 For the model, we used only paired throughfall and soil moisture measurement locations where both top
258 and bottom sensors provided data within the dry periods. All considered potential controlling factors for
259 root water uptake patterns are listed in Table 1. These are daily spatial average soil water storage, the
260 spatial deviation of soil water from the mean, soil water at field capacity and bulk density of the monitored
261 soil layer, number of trees, and number of species within a 5 m radius of each soil moisture location, and
262 inverse distanced basal area (BA) within 5 m radius of each soil moisture location. Basal area was
263 calculated as follows:

$$264 \quad BA_i = \frac{\sum_{R=1}^R W_R A_{tree}}{A} \quad (10)$$

$$265 \quad \text{with } W_R = \frac{(x_i - x_R)^2}{\sum_R (x_i - x_R)^2} \quad (11)$$

266 where i is the soil moisture sensor located at x_i , R is the tree index located at x_R , and A_{tree} is the individual
267 basal area of the corresponding tree, A is the area around the soil moisture sensor i with 5 m in radius.

268 Even though our research plot is a beech-dominated forest, in some spots, two to four species were present
269 within a 5 m radius of the soil moisture sensors.

270 Moreover, we quantified the spatial variability of throughfall as the difference between the throughfall
271 measured at a given location and the spatial mean normalized by the spatial mean. Here we considered
272 this variable at a two-time scales: the week(s) prior to root water uptake estimation period, and the median
273 of the entire measurement period. We also included interaction terms (Table 1) as fixed factors in the
274 model. Because of repeated observations at the measurement locations, soil moisture sensor points and
275 dry periods, (i.e., the root water uptake estimated time interval), were considered as random effects.



276 We conducted all analyses with the R statistical software (R Core Team, 2022) and used the *lmer* function
277 in the 'lme4' package (Bates et al., 2015) for the model development. We visually checked the model
278 assumptions using the 'check_model' function of the 'performance' package (Lüdtke et al., 2021).

279 In addition, we calculated both conditional and marginal R^2 of the model with the 'MuMIn' package
280 (Bartoń, 2020). While the conditional R^2 includes the variance of the entire model, the marginal R^2
281 subsumes only the fixed effects (Bartoń, 2020). Before fitting the linear mixed effects model, we tested
282 for co-linearity of the considered variables and scaled the data with a Z-transformation by using the 'scale'
283 function in base R (R Core Team, 2022), which allowed us to evaluate the individual effect of fixed effects
284 by comparing slopes and significance levels.

285 We developed the optimal model by applying a systematic model selection procedure based on Akaike's
286 Information Criterion (AIC) comparison in combination with the examination of the factors. Model
287 selection began with the beyond-optimal model, which included all possible fixed and random effects.
288 We stepwise evaluated each fixed effect based on its respective significance (p value comparison) by
289 fitting the model the maximum likelihood (ML) to be able to compare AIC values (Zuur et al., 2009). In
290 each step, starting with interaction terms, we identified the least significant effect and formulated a model
291 without it. We compared the AIC values of the model before and after removing the effect, discarding it
292 in case the AIC was unaffected or decreased. We followed the procedure with the next equally detected
293 effect, and repeated it until only significant fixed effects remained, and the model with the lowest AIC
294 (the optimal model) was obtained.

295 As a final step, the best model was refitted with restricted maximum likelihood (REML) (Zuur et al.,
296 2009).

297
298
299
300
301



302
 303

Table 1 List of fixed and random factors considered for estimating the root water uptake patterns through linear mixed effects model. Interaction is shown with ‘x’.

Fixed Factors	
Single Factors	Interaction Factors
Spatial average of soil water storage in the monitored soil layer (\bar{S})	$\bar{S} \times S_{FC}$
Spatial deviation of soil water storage from the mean (δS)	$\delta S \times S_{FC}$
Field capacity of the monitored soil layer (S_{FC})	$\delta S \times BA$
Bulk density capacity of the monitored soil layer (d_{bulk})	$\bar{S} \times BA$
Spatial deviation of throughfall of events measured in sampling week previous to the corresponding dry period ($\delta P_{TF_{last\ ev.}}$)	$\delta S \times n_{tree}$
The median of spatial deviation of throughfall measured within the whole sampling period ($\widehat{\delta P_{TF}}$)	$\bar{S} \times n_{tree}$
Number of trees (n_{tree})	$\delta P_{TF_{last\ ev.}} \times S_{FC}$
Basal area (BA)	$\delta P_{TF_{temp.\ stable.}} \times S_{FC}$
Number of species ($n_{sp,tree}$)	$\delta P_{TF_{last\ ev.}} \times d_{bulk}$
	$\delta P_{TF_{temp.\ stable.}} \times d_{bulk}$
	$n_{sp,tree} \times WA_{int}$
Random factors	
Soil moisture sensor location	
Dry period	

304

3) Results

305

3.1) Spatio-temporal distribution of throughfall and soil water content

306

In 12 out of the 16 sampling weeks, the weekly gross precipitation was more than half of the total potential evapotranspiration. Table 2 further shows the distribution of throughfall sampled in 2019 (April-August)

307

at 200 collectors and the 98 collectors that were paired with soil moisture sensors. The weekly throughfall

308

increased with the increase in rain events. Additionally, the coefficient of quartile variation (CQV) of

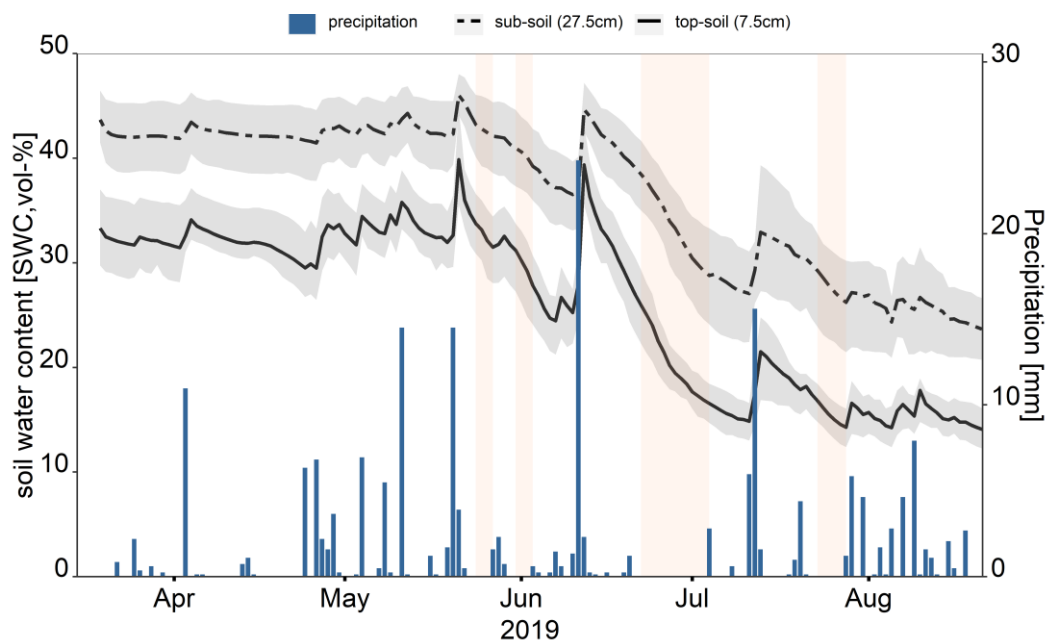
309



310 throughfall was generally lower for larger cumulative weekly rains. On average, the paired collectors
311 received similar amounts of throughfall to all collectors (Table 2). The CQV of data from the paired
312 collectors ranged from 0.27 to 0.6, which is similar to the CQV of throughfall sampled at all collectors.
313 The octile skew (OS_8) of paired and of all collectors was also similar.

314 As the growing season progressed in 2019, the average soil water content decreased in both the topsoil
315 and subsoil. In April and early May, the average volumetric soil water content in the top soil was above
316 30%, which dropped to below 10% by the end of August. In the subsoil, the volumetric soil water content
317 similarly declined from above 40 % to below 20 % over the sampling period (Figure 2). On average, soil
318 water changed from 52.5mm to 17.5 mm in the topsoil and from 80 mm to 40mm in the subsoil.

319 We derived root water uptake for four periods (19 days) under different soil wetness conditions that
320 captured the seasonal variation of soil water content, including late spring when the soil water content
321 was higher, following re-wetting with late summer rains. As listed in Table 3 and shown in Figure 2, two
322 periods were in late May and early June, and each lasted two days. The third period began in late June
323 and lasted 11 days; the last was four days in late July. During these periods, the average soil water content
324 declined from 33 to 15 % in the topsoil and from 43 to 27% in the subsoil. Table 3 additionally shows
325 that within the dry periods, the coefficient of quartile variation (CQV) of soil water content was between
326 0.09 -0.14 and 0.08 to 0.16 in the topsoil and subsoil. During the dry periods, the spatial heterogeneity of
327 soil water content in the subsoil increased systematically. In contrast, the spatial variation of topsoil soil
328 water content did not correlate with soil dryness.



329

330

331

332

333

Figure 2 Soil moisture temporal variation in top and subsoil together with the daily precipitation measured at the nearby Reckenbühl station (approximately 1.4 km to the Northeast). The solid and dashed lines are spatial mean of soil water content estimated based on top (7.5 cm) and bottom (27.5 cm) sensors, and grey shaded areas show first and third quartiles. The reddish shaded areas show defined dry periods within the throughfall sampling when root water uptake could be estimated.

Table 2 Cumulative potential evapotranspiration in mm ($E_{\text{pot,cum}}$), gross precipitation (P_g), the ratio of total precipitation to the potential evapotranspiration, spatial mean of throughfall based on all collectors ($\overline{P_{TF}}$), spatial mean of throughfall based paired collectors ($\overline{P_{TF}}_{\text{paired}}$) in mm, interquartile range (IQR), coefficient of quartile variation (CQV) and octile skewness (OS_8) of both all and paired throughfall collectors during the sampling week. The values are ordered according to the cumulated gross precipitation size.

Date	$E_{\text{pot,cum}}$	P_g	P_g/E_{pot}	$\overline{P_{TF}}$	$\frac{IQR}{\overline{P_{TF}}}$	$\frac{COV}{\overline{P_{TF}}}$	$\frac{OS_8}{\overline{P_{TF}}}$	$\overline{P_{TF}}_{\text{paired}}$	$\frac{IQR}{\overline{P_{TF}}_{\text{paired}}}$	$\frac{CQV}{\overline{P_{TF}}_{\text{paired}}}$	$\frac{OS_8}{\overline{P_{TF}}_{\text{paired}}}$
04-06-2019	13.55	0.76	0.06	0.35	0.18	0.25	0.46	0.34	0.16	0.24	0.49
26-06-2019	20.87	1.73	0.08	0.97	0.44	0.24	0.16	0.98	0.53	0.27	0.27
17-04-2019	5.62	2.42	0.43	1.72	0.27	0.08	0.23	1.72	0.33	0.09	0.09
18-06-2019	9.46	4.00	0.42	2.58	0.62	0.12	-0.03	2.57	0.53	0.10	-0.08
29-05-2019	10.15	6.27	0.62	3.77	1.24	0.17	-0.52	3.63	1.50	0.21	-0.42
24-07-2019	13.52	7.80	0.58	4.61	1.06	0.12	-0.34	4.48	0.88	0.10	-0.63
21-08-2019	8.94	8.54	0.96	5.19	1.06	0.10	-0.47	5.17	0.97	0.10	-0.44
30-07-2019	12.68	10.73	0.85	7.81	2.25	0.15	-1.51	7.58	2.28	0.15	-1.17
07-05-2019	6.65	12.56	1.89	9.21	1.33	0.07	-0.75	9.21	1.99	0.11	-1.05
14-08-2019	8.51	13.79	1.62	11.19	2.65	0.12	-1.40	10.99	2.98	0.13	-1.13
08-08-2019	13.91	23.87	1.72	16.60	2.65	0.08	-1.10	16.52	2.65	0.08	-1.17
30-04-2019	5.93	24.47	4.13	18.44	3.09	0.08	-1.63	18.30	2.65	0.07	-1.23
17-07-2019	8.28	29.27	3.54	24.22	3.54	0.07	-2.08	24.39	3.54	0.07	-2.59
15-05-2019	7.42	29.53	3.98	22.10	3.54	0.08	-2.11	22.21	3.54	0.08	-2.11
22-05-2019	6.74	41.82	6.20	30.94	3.54	0.06	-3.04	30.54	3.54	0.06	-3.46
13-06-2019	14.47	71.84	4.96	57.77	8.51	0.07	-5.82	57.99	7.29	0.06	-6.52



335 **Table 3** The spatial average of daily volumetric soil water content ($\overline{\theta_{\text{top-soil}}}$, vol-%) in topsoil (0-17.5 cm), and ($\overline{\theta_{\text{subsoil}}}$, vol-%)
 336 in subsoil (17.5 – 37.5 cm) during the defined dry periods. The inter quartile range (IQR), and coefficient of quartile variation
 337 (CQV) of daily volumetric soil water content in both layers during the dry periods.

Date	$\overline{\theta_{\text{top-soil}}}$ (vol-%)	IQR $\theta_{\text{top-soil}}$ (vol-%)	CQV $\theta_{\text{top-soil}}$ (vol-%)	$\overline{\theta_{\text{sub-soil}}}$ (vol-%)	IQR θ_{subsoil} (vol-%)	CQV θ_{subsoil} (vol-%)	Dry Period
25-05-2019	33.17	5.72	0.09	42.82	6.72	0.08	1
26-05-2019	32.12	6.62	0.10	42.46	6.67	0.08	1
01-06-2019	30.23	6.87	0.12	40.61	6.9	0.09	2
02-06-2019	29.22	7.23	0.13	40.11	6.85	0.09	2
23-06-2019	25.01	6.69	0.14	37.80	6.38	0.08	3
24-06-2019	24.04	6.45	0.14	36.94	6.22	0.08	3
25-06-2019	22.52	5.43	0.12	36.13	6.54	0.09	3
26-06-2019	21.48	5.07	0.12	35.24	6.71	0.10	3
27-06-2019	20.20	4.25	0.11	33.98	7.75	0.12	3
28-06-2019	19.45	3.85	0.10	33.31	8.08	0.12	3
29-06-2019	18.98	3.83	0.10	32.36	8.05	0.12	3
30-06-2019	18.44	3.52	0.09	31.37	8.15	0.13	3
01-07-2019	17.67	3.62	0.10	30.45	8.18	0.13	3
02-07-2019	17.29	4.18	0.12	29.84	8.87	0.15	3
03-07-2019	16.89	3.72	0.11	29.26	8.98	0.15	3
24-07-2019	16.15	3.48	0.11	28.56	8.7	0.16	4
25-07-2019	15.51	3.47	0.11	27.85	8.67	0.16	4
26-07-2019	14.98	3.57	0.12	27.21	8.49	0.16	4
27-07-2019	14.57	3.65	0.13	26.65	8.63	0.16	4

338

339 3.2) Soil water storage, potential evapotranspiration, and root water uptake

340 The integrated field capacity of the monitored soil depth was 160 mm on average at the research site.
 341 Table 4 shows that soil water storage was much lower than the field capacity during the dry periods, and
 342 the mean soil water storage dropped below 42 mm in late July. In addition, Table 4 demonstrates that the
 343 average root water uptake (\overline{E}_t) ranged from 0.94 mm d⁻¹ to 3 mm d⁻¹ while potential evapotranspiration
 344 (E_{pot}) ranged from 1.75 mm d⁻¹ to 3.12 mm d⁻¹. The discrepancy between average root water uptake and
 345 the potential evapotranspiration increased as soil water storage assessed by the soil sensors progressively
 346 decreased, especially during the longest dry period (Table 4). Root water uptake showed greater spatial
 347 variation than water input and soil wetness. The coefficient of quartile variation (CQV) of root water
 348 uptake ranged from 0.15 to 0.28, which was higher than the CQV of throughfall and volumetric soil water
 349 content in both soil layers.

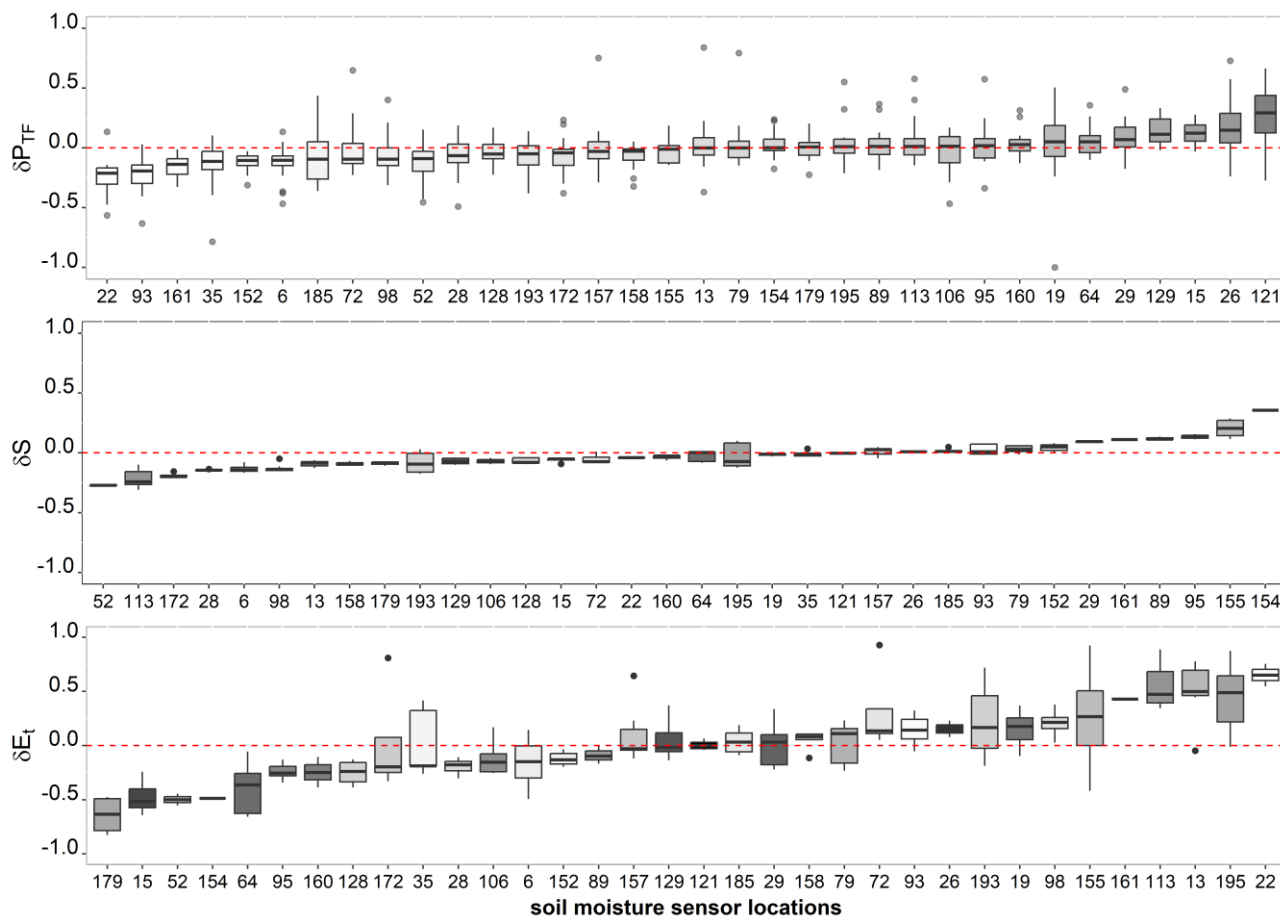


350 **Table 4** The daily average air temperature (T_{air} , °C), potential evapotranspiration (E_{pot} , mm), mean soil water storage (\bar{S} , mm)
 351 in monitored soil layer (0 - 37.5 cm), and spatial mean of daily root water uptake (\bar{E}_t , mm) based on all soil moisture sensors,
 352 and the ratio of the root water uptake to the potential evapotranspiration together with and standard deviation (SD) and
 353 coefficient of quartile variation (CQV) of the daily root water uptake during the defined dry periods

Date	T_{air} (°C)	E_{pot} (mm)	\bar{S} (mm)	\bar{E}_t (mm)	$\bar{E}_t / E_{\text{pot}}$ (%)	SD \bar{E}_t	CQV \bar{E}_t	Dry Period
25-05-2019	12.74	1.80	71.94	1.09	60.56	0.38	0.28	1
26-05-2019	14.43	1.90	70.57	1.30	68.42	0.48	0.25	1
01-06-2019	18.42	2.59	67.16	2.26	87.26	0.98	0.27	2
02-06-2019	21.38	2.77	65.79	2.50	90.25	1.12	0.18	2
23-06-2019	19.45	2.79	59.81	2.83	101.43	0.90	0.19	3
24-06-2019	20.22	2.82	58.16	2.62	92.91	0.76	0.17	3
25-06-2019	22.52	2.89	55.96	2.67	92.39	0.78	0.16	3
26-06-2019	25.73	2.96	54.13	3.00	101.35	0.88	0.15	3
27-06-2019	18.83	2.75	51.91	2.28	82.91	0.55	0.16	3
28-06-2019	16.07	2.58	50.55	1.53	59.30	0.40	0.20	3
29-06-2019	19.59	2.85	49.55	2.11	74.04	0.60	0.20	3
30-06-2019	25.54	3.12	48.26	2.57	82.37	0.86	0.18	3
01-07-2019	20.63	2.30	46.69	1.59	69.13	0.53	0.18	3
02-07-2019	14.88	1.75	45.81	1.08	61.71	0.42	0.24	3
03-07-2019	13.77	1.91	44.95	0.94	49.21	0.30	0.23	3
24-07-2019	24.39	2.76	43.61	1.88	68.12	0.64	0.19	4
25-07-2019	25.33	2.82	42.31	1.77	62.77	0.60	0.24	4
2019-07-26	23.27	2.64	41.18	1.40	53.03	0.55	0.18	4
2019-07-27	21.29	2.68	40.23	1.21	45.15	0.47	0.19	4

354 3.3) Soil water, throughfall, and root water uptake patterns

355 At soil moisture measurement points where daily root water uptake was determined ($n = 34$), we
 356 calculated the spatial deviation from the median of throughfall, soil water storage, and root water uptake
 357 to illustrate the spatial patterns. Figure 3 separately shows that some locations received repeatedly less
 358 (or more) throughfall than average ($\delta P_{TF} < 0$) throughout the sampling season. Similarly, some locations,
 359 either stored less water in the soil, i.e., were drier ($\delta S < 0$), and some places had lower root water uptake
 360 (δE_t) or higher than average water uptake throughout the sampling period. However, these locations were
 361 not related to each other. In fact, Figure 3 demonstrates that neither throughfall nor soil water patterns are
 362 directly correlated with the root water uptake patterns. For example, the locations with higher water
 363 uptake were not coupled with elevated throughfall input (locations colored dark) or higher soil water
 364 storage. In addition, soil water storage patterns were not correlated with throughfall patterns.



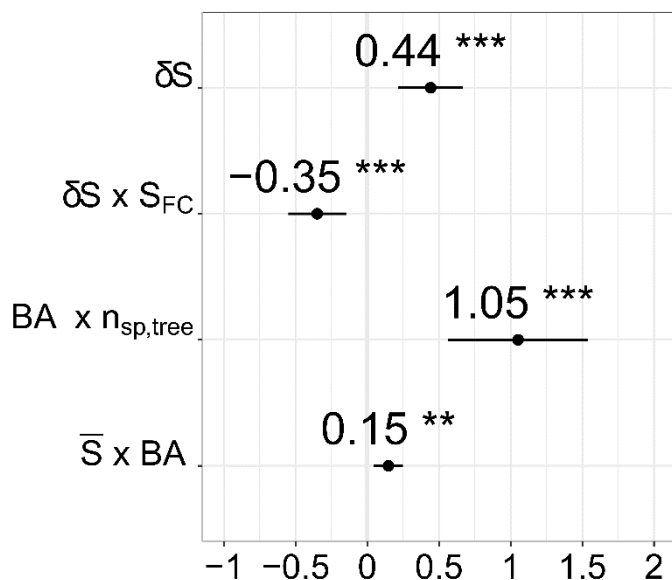
365

366 **Figure 3** Temporal stability of throughfall patterns which is estimated by the spatial deviation from the mean (δP_{TF}) throughout
367 the sampling period in 2019 (April-August), soil water (δS) and root water uptake (δE_r) based on the spatial deviation from
368 the mean during the defined dry periods. Soil moisture sensor locations colored according to throughfall input.

369 **3.5) Fixed factors regulating root water uptake patterns**

370 We used a linear mixed effects model to disentangle the effects of throughfall, soil water, soil properties,
371 and the neighbouring tree characteristics on root water uptake patterns. The fixed and random effects
372 contributed almost equally to the model. The R^2 of the model was 0.77, and the contribution of the fixed
373 effect to the R^2 was 0.39 (See the supplement for more details on the optimal model).

374 Figure 4 shows only the significant fixed effects for root water uptake patterns. Spatial deviation of soil
375 water from the mean (i.e., soil water patterns) was the only single and the most significant factor positively
376 related to the spatial deviation of root water uptake. Thus, water uptake was elevated at locations where
377 the most water was retained in the soil at the given time, i.e., greater soil water storage.



378

379 **Figure 4** The significant fixed factors of the best model to estimate root water uptake patterns (δE_i). Values on the x-axis
380 indicate the slope of the relations. All variables were scaled by Z-transformation. Interaction is shown with 'x'. Here δS is the
381 spatial deviation of soil water, S_{FC} is the field capacity, $n_{sp,tree}$ is the number of species, BA is the basal area, and \bar{S} is soil water
382 storage. Significance codes are *** $\cong 0$, ** $\cong 0.001$. (the details on the model can be found in the supplement)

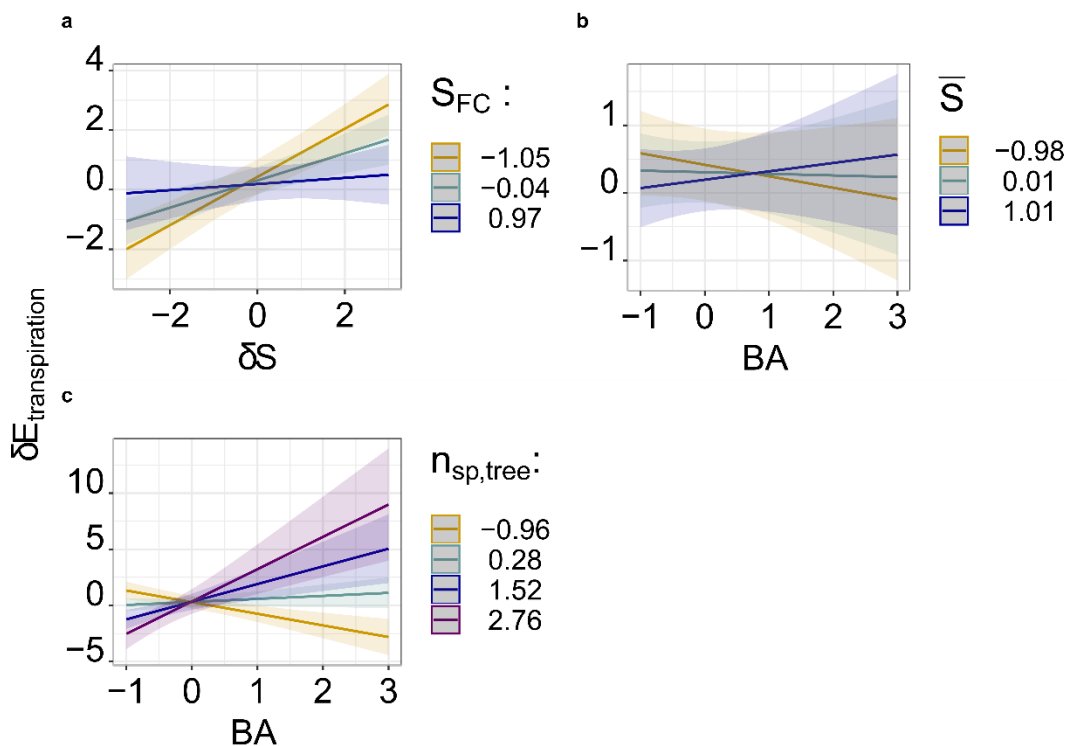
383

384 Field capacity by itself was not a significant factor affecting local root water uptake. However, it strongly
385 influenced how local soil water-controlled root water uptake as a part of the significant interaction term.
386 Figure 5a illustrates how to root water uptake was more dependent on local soil water when field capacity
387 was low (i.e., higher macroporosity). In contrast, soil bulk density and therefore total porosity was not
388 part of the final model.

389 Although the spatial average of soil water storage, e.g., the state of wetness, was not an important factor
390 for local root water uptake by itself, it moderated the impact of basal area (BA) on the spatial distribution
391 of water uptake. We found that as the plot dries, uptake shifts from places with higher to places with lower
392 basal area (Figure 5b). Furthermore, the statistical model revealed that water uptake increased with the
393 higher basal area at locations where multiple species co-existed (Figure 5c). However, the number of
394 species and the basal area were individually not significant fixed effects. Lastly, throughfall patterns were
395 not significant predictors of local root water uptake. Only the median of the spatial deviation of



396 throughfall, which represents temporally stable patterns within the sampling period ($\delta\overline{P}_{TF}$), marginally
397 improved the final model.



398
399 **Figure 5** Visualisation of the significant relations shown in Figure 4, representing the significant drivers of root water uptake
400 patterns during the defined dry periods. Relation to (a) interactive relation of the spatial deviation of soil water storage and
401 field capacity (S_{FC}), (b) the interactive relation of basal area (BA) and the spatial average of soil water storage (\overline{S}), (c) the
402 interactive relation of number of species ($n_{sp,tree}$) and basal area (BA.).

403 4) Discussion

404 4.1) Spatial variation in throughfall does not affect root water uptake patterns

405 We adequately captured the spatial distribution and temporal stability of throughfall at locations where
406 local root water uptake was derived. Consistent with previous observations in temperate forests (e.g.,
407 Whelan and Anderson, 1996; Staelens et al., 2006; Metzger et al., 2017), the amount of weekly rainfall
408 significantly altered the spatial distribution of throughfall such that more rainfall, and thus more
409 throughfall, resulted in less spatial variability. Previous studies repeatedly showed that throughfall
410 patterns exhibit temporal stability in forest ecosystems (e.g., Keim et al., 2005; Staelens et al., 2006;



411 Wullaert et al., 2009; Rodrigues et al., 2022). At the same research site, using event-based sampling,
412 Metzger et al., (2017) and Fischer et al., (2023) demonstrated that throughfall patterns persist over time,
413 which was not different in our weekly sampling in 2019. With canopy cover being the key driver of
414 throughfall (Fischer et al., 2023), it is not surprising that weekly cumulative events resulted in a localized
415 high and low throughfall input.

416 Contrary to expectations (Bouten et al., 1992; Guswa and Spence, 2012; Coenders-Gerrits et al., 2013;
417 Fischer et al., 2023), our results showed that throughfall hotspots do not increase or facilitate greater root
418 water uptake. In addition, the linear mixed effects model results confirmed that throughfall patterns do
419 not drive the variation in root water uptake. We attributed the absence of this to two reasons: (1) decoupled
420 soil water and throughfall patterns, (2) non-water limited conditions.

421 Regarding (1), we confirmed that the temporally stable throughfall patterns do not correspond to the post-
422 event soil water and root water uptake patterns. We paired the measurements of throughfall and soil water
423 content measurements – and thus the estimates of root water uptake- within a distance of 1 m. The spatial
424 correlation length of soil water content and throughfall is on the order of 6-10 m in natural temperate
425 forests (Keim et al., 2005; Gerrits et al., 2010; Zehe et al., 2010). In the same study site with the spatially
426 extended throughfall sampling, Fischer et al., (2023) found that the throughfall correlation length
427 increased with decreasing event size, varying from 6.2 m to 9.5 m depending on the size of the rain events.
428 Thus, the paired sampling design in our study likely provided co-located throughfall and soil moisture
429 measurements. Nevertheless, only locations that stored more water than average rarely corresponded with
430 the elevated throughfall input without a significant correlation. Hence, variation in soil water storage was
431 not related to throughfall patterns despite temporally persistent local high and low throughfall inputs.

432 On the one hand, some studies, mostly conducted in the arid regions and coniferous forests, reported that
433 soil wetting patterns were not or only partly linked to throughfall variation, despite recurrent throughfall
434 patterns (Raat et al., 2002; Shachnovich et al., 2008; Zhu et al., 2021). Forest floor thickness, horizontal
435 water flow, and soil properties were suggested as reasons for the decoupled patterns. On the other hand,
436 some modeling and field studies conducted in temperate deciduous forests found that throughfall patterns
437 influenced soil moisture response rather than soil water storage variability (Coenders-Gerrits et al., 2013;
438 Metzger et al., 2017; Fischer et al., 2023). In those studies, possible reasons were attributed to local



439 processes such as preferential flow due to soil water repellency, the soil pore structure, or elevated root
440 water uptake. Our results support that it is not root water uptake but preferential flow paths that likely
441 decouples the throughfall and soil water patterns. In fact, Fischer et al., (2023) using independent
442 throughfall and soil water content sampling designs, demonstrated that the signature of throughfall
443 patterns dissipated in the post-event soil water variation. However, they detected the stronger influence
444 of throughfall patterns in the soil moisture response to rainfall in the 2015 and 2016 growing seasons. The
445 temporal variation in soil water content in the 2019 growing season was similar to the seasonal decline in
446 soil water content in 2015 (Metzger et al., 2017). Dry soil conditions can lead to rapid drainage due to
447 reduced water holding capability (Jost et al., 2004; Blume et al., 2009; Wiekenkamp et al., 2016; Demand
448 et al., 2019; Molina et al., 2019) regardless of throughfall amount and its variation. Therefore, our findings
449 support that the localized throughfall input likely enhances preferential flow because of low soil retention
450 (Fischer et al., 2023) rather than local root water uptake.

451 As a result, the fast flow processes likely dominate how water is stored and transported at our site, erasing
452 the throughfall distribution signature in soil water and root water uptake patterns. Our results also support
453 that the spatial variation of throughfall affects drainage and subsurface flow (Keim et al., 2006; Blume et
454 al., 2009; Guswa and Spence, 2012), and root activity does not alter canopy-attributed heterogeneity in
455 drainage pathways (Guswa, 2012).

456 The second reason (2) is related to water-limitation conditions. In central Europe, 2019 was the second
457 consecutive extremely dry summer (Boergens et al., 2020), which damaged beech forests (Obladen et al.,
458 2021). On average, however, the potential evapotranspiration demand was met at the study site despite
459 the low soil water storage. The ratio of root water uptake to potential evapotranspiration was mostly above
460 65%, which is within the expected range even in the absence of shallow groundwater storage (Nie et al.,
461 2021). Hence, local biotic and abiotic factors determined the spatial variation of root water uptake during
462 growing season rather than throughfall patterns. However, the discrepancy between daily potential
463 evapotranspiration and root water uptake only increased as the soil in the sampled layers dried out,
464 possibly due to a potential shift in the water uptake depth (see below).



465 **4. 2) Relative and average soil wetness shapes root water uptake patterns**

466 We found that spatial variation in soil water storage strongly regulates local water uptake such that wetter
467 locations enhance root water uptake. This finding is in line with expectations as transpiration rate relies
468 on soil water availability and distribution (Couvreur et al., 2014; Klein et al., 2014; Hildebrandt et al.,
469 2016). Here, our results provide further support that root water uptake is likely to reduce the spatial
470 variability in soil water storage as has been previously suggested (Hopmans and Bristow, 2002; Ivanov
471 et al., 2010; Neumann and Cardon, 2012).

472 For a given meteorological condition, root-water uptake at a particular location is a function of water
473 transport resistance between root and soil in addition to the soil-water potential (Cardon and Letey, 1992;
474 Shani and Dudley, 1996; Lhomme, 1998). Both characteristics depend on local soil texture and soil
475 moisture, and the latter in turn is affected by the local rate of uptake. Although bulk density is attributed
476 to porous space and eventually water retention (Zacharias and Wessolek, 2007; Looy et al., 2017), we
477 surprisingly found that the bulk density of the monitored soil layer did not affect local water uptake. In
478 contrast, the combination of higher field capacity and low soil water probably hindered the local water
479 uptake due to lower soil water retention. Differences in local soil properties regulate matric potential at a
480 certain soil wetness. Thus, our result indicates that wetter locations may not always correspond to the
481 same degree of matric potential and ease root water uptake due to the local field capacity. However, our
482 findings suggest that solely soil properties were less important than other tested variables despite their
483 control on the spatial distribution of soil moisture (Vereecken et al., 2022) and water accessibility for
484 transpiration (Vereecken et al., 2007; Cai et al., 2018).

485 In addition, the spatial mean of soil water affected root water uptake patterns, yet the effect depended on
486 the basal area, i.e., the size of neighboring trees. We found that as the study site dries out, local water
487 uptake increased in locations with smaller basal areas. Conversely, wetter site conditions facilitate greater
488 water uptake at locations with higher basal areas, i.e., dense clusters of or large trees. We interpret this as
489 a sign that larger trees are likely to shift their water uptake to deeper soil layers to meet transpiration
490 demands, beyond the monitored soil depth (37 cm), as follows: Higher basal area likely increases
491 transpiration demand and enhances water uptake as long as water is available. At the same time, locations
492 with higher basal area exhaust the water storage faster but are able to shift uptake to deeper layers where



493 soil water content is not measured in our monitoring setup. Beech trees have extensive root systems at
494 shallower depths similar to other temperate tree species, such as European ash and sycamore maple
495 (Kreuzwieser and Gessler, 2010; Brinkmann et al., 2019). However, in response to declining soil water
496 content in the topsoil, temperate tree species can tap water from the deeper soil layers (Brinkmann et al.,
497 2019; Agee et al., 2021; Seeger and Weiler, 2021) despite their shallow root system (Leuschner, 2020).
498 Recently, Agee et al. (2021) used a three-dimensional water uptake model based on observations in
499 temperate mixed-deciduous forest to show that water uptake is shifted to the deeper soil layers as soil
500 moisture depletes, which is consistent with the field observations. Also, Krämer and Hölscher (2010)
501 observed in beech and mixed deciduous stands that roots can extract water at depths down to 70 cm soil
502 depth. Similarly, to our site, theirs had a shallow soil layer underlain by weathered limestone.

503 **4.3) Tree species richness regulates root water uptake patterns**

504 In addition to the basal area, we included the number of species and number of tree individuals in the
505 linear mixed effects analysis to explore further the biotic drivers of root water uptake patterns. While the
506 number of trees was unimportant, the number of species and the basal area, showed a significant
507 interaction effect on the local water uptake. The result indicates that an increase in species richness leads
508 to greater root water uptake, depending on the size and/or density of the neighboring trees: Higher basal
509 area, combined with more species, elevates water uptake. In other words, the interactions among
510 neighboring tree species strongly determine root water uptake patterns, and at the same basal area more
511 water can be taken up in a diverse compared to a less diverse neighborhood.

512 In temperate forests, transpiration has been observed to change with tree species richness at the stand
513 level (Krämer and Hölscher, 2010; Gebauer et al., 2012; Kunert et al., 2012; Meißner et al., 2012;
514 Forrester, 2014). Although some studies indicate a positive relationships between tree diversity and water
515 uptake rate (Forrester et al., 2010; Krämer and Hölscher, 2010; Kunert et al., 2012), tree species diversity
516 is not always positively related to water uptake. While Krämer and Hölscher (2010) observed a positive
517 correlation between water uptake and species richness of the plots in the upper soil layers during soil
518 drying in 2006 at the same study site, Meißner et al. (2012) found no relationship between tree diversity
519 and root water uptake in 2009. They attributed this finding to wetter soil conditions. In contrast, Lübke et



520 al. (2016) observed a weak effect of diversity on transpiration in wetter soil conditions but not in drier
521 conditions compared to previous studies (e.g., Pretzsch et al., 2013; del Río et al., 2014). Shortage of
522 water can inflate competition mechanisms for water among tree species (González de Andrés et al., 2018;
523 Vitali et al., 2018; Magh et al., 2020). Our results can be used to show that competition between
524 neighboring tree species increases water uptake capacity at more diverse spots (Wambsganss et al., 2021).
525 In addition, different co-existing tree species can facilitate resource uptake or reduce competition,
526 depending on the temporal and spatial availability of the sources, which is often defined as
527 complementarity (Forrester and Bauhus, 2016). As reviewed and listed by Silvertown et al. (2015),
528 several studies suggest that co-existing tree species reduce competition for subsurface water sources by
529 adopting different vertical root water uptake strategies, referred to as hydrological niche partitioning. In
530 addition, trees can transport water from moist to dry parts of the soil layers through their roots (Neumann
531 and Cardon, 2012). The mechanism is called hydraulic redistribution or hydraulic lift, which can provide
532 water availability to the shallow roots in drier layers (Burgess et al., 1998; Jonard et al., 2011; Hafner et
533 al., 2017; Lee et al., 2018; Rodríguez-Robles et al., 2020; Hafner et al., 2021). Hafner et al. (2021) found
534 in an experiment with six temperate tree species, including the European beech, that the neighboring tree
535 species diversity may not be important for exploiting water uptake through hydraulic redistribution. Both
536 hydraulic niche partitioning and redistribution have been observed vertically, whereas horizontal patterns
537 are largely unexplored in the context of niche partitioning (Hildebrandt, 2020). Our results do not provide
538 direct evidence for either hydraulic redistribution or horizontal niche partitioning. However, they indicate
539 that horizontal root water uptake patterns are regulated by species richness.

540 **5) Conclusion**

541 We investigated the factors that influence the spatial patterns of root water uptake by considering
542 heterogeneity in throughfall and soil water. To that end, we acquired a comprehensive data set based on
543 throughfall measurements paired with soil moisture sensors in a mixed deciduous forest. Soil and
544 neighboring tree characteristics were also included in the linear mixed effects model. We found that
545 variation in root water uptake did not correspond to throughfall. Wetter soil locations, poorly associated



546 with higher throughfall, increased local root water uptake. In contrast, how average soil water conditions
547 modified root water uptake depended on the neighborhood basal area. As the site dried out, large trees
548 likely took up water in deeper layers to meet transpiration demands. Furthermore, an increase in species
549 diversity promoted root water uptake, similarly depending on the size of neighboring trees, suggesting
550 active complementarity mechanisms in the forest stand. In conclusion, our results suggest that soil water
551 distribution and neighboring tree characteristics regulate root water uptake patterns more than soil
552 properties and throughfall variation.

553

554 **Acknowledgments**

555 This study is part of the Collaborative Research Centre (CRC 1076 AquaDiva) of the Friedrich Schiller
556 University Jena, funded by the Deutsche Forschungsgemeinschaft (DFG, German Research
557 Foundation)—SFB 1076—Project Number 218627073. We thank to AquaDiva subproject D03 for
558 weather station (Reckenbuel) data. Also, people who contributed to installation of soil moisture sensors
559 in the research site: Ricardo Ontiveros-Enriques, Bernd Ruppe, Danny Schelhorn, Josef Weckmüller. We
560 thank the Hainich CZE site manager Robert Lehmann and the Hainich National Park. We thank the
561 bachelor and master students Carla Peter, Xiaoyu Zhao, Stephan Bock for their contribution to throughfall
562 sampling.

563

564 **Data availability**

565 The dataset is currently being prepared for publication in an official repository. The DOI will be published
566 with the data at the latest when the data are published.

567

568 **Author contributions**

569 GD and AH designed the throughfall measurement setup, AH and JCM designed soil moisture
570 measurement. GD conducted the field sampling with assistance from JF and the students listed in the
571 Acknowledgments. GD analyzed the data, developed the linear mixed effects model, and analyzed the
572 results with AH and AG. GD prepared the first version of the manuscript, and all authors contributed to
573 discussions and the final version of the manuscript.



574 **Competing interests**

575 Anke Hildebrandt is part of the editorial board of HESS. The peer-review process was guided by an
576 independent editor, and the authors have also no other competing interests to declare.

577

578 **6) References**

579 Agee, E., He, L., Bisht, G., Couvreur, V., Shahbaz, P., Meunier, F., Gough, C. M., Matheny, A. M.,
580 Bohrer, G., and Ivanov, V.: Root lateral interactions drive water uptake patterns under water limitation,
581 *Advances in Water Resources*, 151, 103896, <https://doi.org/10.1016/j.advwatres.2021.103896>, 2021.

582 Bachmair, S., Weiler, M., and Troch, P. A.: Intercomparing hillslope hydrological dynamics: Spatio-
583 temporal variability and vegetation cover effects, *Water Resources Research*, 48,
584 <https://doi.org/10.1029/2011WR011196>, 2012.

585 Baroni, G., Ortuani, B., Facchi, A., and Gandolfi, C.: The role of vegetation and soil properties on the
586 spatio-temporal variability of the surface soil moisture in a maize-cropped field, *Journal of Hydrology*,
587 489, 148–159, <https://doi.org/10.1016/j.jhydrol.2013.03.007>, 2013.

588 Bartoń, K.: MuMIn: Multi-Model Inference, 2020.

589 Bates, D., Mächler, M., Bolker, B., and Walker, S.: Fitting Linear Mixed-Effects Models Using **lme4**, *J.*
590 *Stat. Soft.*, 67, <https://doi.org/10.18637/jss.v067.i01>, 2015.

591 Blume, T., Zehe, E., and Bronstert, A.: Use of soil moisture dynamics and patterns at different spatio-
592 temporal scales for the investigation of subsurface flow processes, *Hydrology and Earth System Sciences*,
593 13, 1215–1233, <https://doi.org/10.5194/hess-13-1215-2009>, 2009.

594 Boergens, E., Güntner, A., Dobsław, H., and Dahle, C.: Quantifying the Central European Droughts in
595 2018 and 2019 With GRACE Follow-On, *Geophysical Research Letters*, 47, e2020GL087285,
596 <https://doi.org/10.1029/2020GL087285>, 2020.

597 Bogena, H. R., Herbst, M., Huisman, J. A., Rosenbaum, U., Weuthen, A., and Vereecken, H.: Potential
598 of Wireless Sensor Networks for Measuring Soil Water Content Variability, *Vadose Zone Journal*, 9,
599 1002–1013, <https://doi.org/10.2136/vzj2009.0173>, 2010.

600 Borchers, H. W.: *pracma: Practical Numerical Math Functions*, 2021.



- 601 Bouten, W., Heimovaara, T. J., and Tiktak, A.: Spatial patterns of throughfall and soil water dynamics in
602 a Douglas fir stand, *Water Resources Research*, 28, 3227–3233, <https://doi.org/10.1029/92WR01764>,
603 1992.
- 604 Brinkmann, N., Eugster, W., Buchmann, N., and Kahmen, A.: Species-specific differences in water
605 uptake depth of mature temperate trees vary with water availability in the soil, *Plant Biology*, 21, 71–81,
606 <https://doi.org/10.1111/plb.12907>, 2019.
- 607 Brum, M., Vadeboncoeur, M. A., Ivanov, V., Asbjornsen, H., Saleska, S., Alves, L. F., Penha, D., Dias,
608 J. D., Aragão, L. E. O. C., Barros, F., Bittencourt, P., Pereira, L., and Oliveira, R. S.: Hydrological niche
609 segregation defines forest structure and drought tolerance strategies in a seasonal Amazon forest, *Journal*
610 *of Ecology*, 107, 318–333, <https://doi.org/10.1111/1365-2745.13022>, 2019.
- 611 Burgess, S. S. O., Adams, M. A., Turner, N. C., and Ong, C. K.: The redistribution of soil water by tree
612 root systems, *Oecologia*, 115, 306–311, <https://doi.org/10.1007/s004420050521>, 1998.
- 613 Cai, G., Vanderborcht, J., Langensiepen, M., Schnepf, A., Hüging, H., and Vereecken, H.: Root growth,
614 water uptake, and sap flow of winter wheat in response to different soil water conditions, *Hydrol. Earth*
615 *Syst. Sci.*, 22, 2449–2470, <https://doi.org/10.5194/hess-22-2449-2018>, 2018.
- 616 Cardon, G. E. and Letey, J.: Plant Water Uptake Terms Evaluated for Soil Water and Solute Movement
617 Models, *Soil Science Society of America Journal*, 56, 1876–1880,
618 <https://doi.org/10.2136/sssaj1992.03615995005600060038x>, 1992.
- 619 Carlyle-Moses, Darryl. E., Lishman, Chad. E., and McKee, Adam. J.: A preliminary evaluation of
620 throughfall sampling techniques in a mature coniferous forest, *Journal of Forestry Research*, 25, 407–
621 413, <https://doi.org/10.1007/s11676-014-0468-8>, 2014.
- 622 Coenders-Gerrits, A. M. J., Hopp, L., Savenije, H. H. G., and Pfister, L.: The effect of spatial throughfall
623 patterns on soil moisture patterns at the hillslope scale, *Hydrol. Earth Syst. Sci.*, 17, 1749–1763,
624 <https://doi.org/10.5194/hess-17-1749-2013>, 2013.
- 625 Cosh, M. H., Jackson, T. J., Moran, S., and Bindlish, R.: Temporal persistence and stability of surface
626 soil moisture in a semi-arid watershed, *Remote Sensing of Environment*, 112, 304–313,
627 <https://doi.org/10.1016/j.rse.2007.07.001>, 2008.
- 628 Couvreur, V., Vanderborcht, J., Beff, L., and Javaux, M.: Horizontal soil water potential heterogeneity:
629 simplifying approaches for crop water dynamics models, *Hydrology and Earth System Sciences*, 18,
630 1723–1743, <https://doi.org/10.5194/hess-18-1723-2014>, 2014.
- 631 Crockford, R. H. and Richardson, D. P.: Partitioning of rainfall into throughfall, stemflow and
632 interception: effect of forest type, ground cover and climate, *Hydrological Processes*, 14, 2903–2920,
633 2000.



- 634 Demand, D., Blume, T., and Weiler, M.: Spatio-temporal relevance and controls of preferential flow at
635 the landscape scale, *Hydrol. Earth Syst. Sci.*, 23, 4869–4889, <https://doi.org/10.5194/hess-23-4869-2019>,
636 2019.
- 637 Demir, G., Michalzik, B., Filipzik, J., Metzger, J., and Hildebrandt, A.: Spatial variation of grassland
638 canopy affects soil wetting patterns and preferential flow,
639 <https://doi.org/10.22541/au.164970545.54927607/v1>, 2022.
- 640 Dunkerley, D.: Stemflow on the woody parts of plants: dependence on rainfall intensity and event profile
641 from laboratory simulations, *Hydrological Processes*, 28, 5469–5482, <https://doi.org/10.1002/hyp.10050>,
642 2014.
- 643 Emerman, S. H. and Dawson, T. E.: Hydraulic Lift and Its Influence on the Water Content of the
644 Rhizosphere: An Example from Sugar Maple, *Acer saccharum*, *Oecologia*, 108, 273–278, 1996.
- 645 Fan, J., Oestergaard, K. T., Guyot, A., Jensen, D. G., and Lockington, D. A.: Spatial variability of
646 throughfall and stemflow in an exotic pine plantation of subtropical coastal Australia, *Hydrological
647 Processes*, 29, 793–804, <https://doi.org/10.1002/hyp.10193>, 2015.
- 648 Fischer, C., Metzger, J. C., Demir, G., Wutzler, T., and Hildebrandt, A.: Throughfall spatial patterns
649 translate into spatial patterns of soil moisture dynamics – empirical evidence, *Ecohydrology/Instruments
650 and observation techniques*, <https://doi.org/10.5194/hess-2022-418>, 2023.
- 651 Forrester, D. I.: The spatial and temporal dynamics of species interactions in mixed-species forests: From
652 pattern to process, *Forest Ecology and Management*, 312, 282–292,
653 <https://doi.org/10.1016/j.foreco.2013.10.003>, 2014.
- 654 Forrester, D. I. and Bauhus, J.: A Review of Processes Behind Diversity—Productivity Relationships in
655 Forests, *Curr Forestry Rep*, 2, 45–61, <https://doi.org/10.1007/s40725-016-0031-2>, 2016.
- 656 Forrester, D. I., Theiveyanathan, S., Collopy, J. J., and Marcar, N. E.: Enhanced water use efficiency in a
657 mixed *Eucalyptus globulus* and *Acacia mearnsii* plantation, *Forest Ecology and Management*, 259, 1761–
658 1770, <https://doi.org/10.1016/j.foreco.2009.07.036>, 2010.
- 659 Gebauer, T., Horna, V., and Leuschner, C.: Canopy transpiration of pure and mixed forest stands with
660 variable abundance of European beech, *Journal of Hydrology*, 442–443, 2–14,
661 <https://doi.org/10.1016/j.jhydrol.2012.03.009>, 2012.
- 662 Gerrits, A. M. J., Pfister, L., and Savenije, H. H. G.: Spatial and temporal variability of canopy and forest
663 floor interception in a beech forest, *Hydrol. Process.*, 24, 3011–3025, <https://doi.org/10.1002/hyp.7712>,
664 2010.



- 665 González de Andrés, E., Camarero, J. J., Blanco, J. A., Imbert, J. B., Lo, Y.-H., Sangüesa-Barreda, G.,
666 and Castillo, F. J.: Tree-to-tree competition in mixed European beech–Scots pine forests has different
667 impacts on growth and water-use efficiency depending on site conditions, *Journal of Ecology*, 106, 59–
668 75, <https://doi.org/10.1111/1365-2745.12813>, 2018.
- 669 Grayson, R. B., Western, A. W., Chiew, F. H. S., and Blöschl, G.: Preferred states in spatial soil moisture
670 patterns: Local and nonlocal controls, *Water Resources Research*, 33, 2897–2908,
671 <https://doi.org/10.1029/97WR02174>, 1997.
- 672 Guderle, M. and Hildebrandt, A.: Using measured soil water contents to estimate evapotranspiration and
673 root water uptake profiles – a comparative study, *Hydrol. Earth Syst. Sci.*, 17, 2015.
- 674 Guderle, M., Bachmann, D., Milcu, A., Gockele, A., Bechmann, M., Fischer, C., Roscher, C., Landais,
675 D., Ravel, O., Devidal, S., Roy, J., Gessler, A., Buchmann, N., Weigelt, A., and Hildebrandt, A.: Dynamic
676 niche partitioning in root water uptake facilitates efficient water use in more diverse grassland plant
677 communities, *Funct Ecol*, 32, 214–227, <https://doi.org/10.1111/1365-2435.12948>, 2018.
- 678 Guo, J. S., Hungate, B. A., Kolb, T. E., and Koch, G. W.: Water source niche overlap increases with site
679 moisture availability in woody perennials, *Plant Ecol*, 219, 719–735, <https://doi.org/10.1007/s11258-018-680-0829-z>, 2018.
- 681 Guswa, A. J.: Canopy vs. Roots: Production and Destruction of Variability in Soil Moisture and
682 Hydrologic Fluxes, *Vadose Zone Journal*, 11, vzj2011.0159, <https://doi.org/10.2136/vzj2011.0159>, 2012.
- 683 Guswa, A. J. and Spence, C. M.: Effect of throughfall variability on recharge: application to hemlock and
684 deciduous forests in western Massachusetts, *Ecohydrology*, 5, 563–574, <https://doi.org/10.1002/eco.281>,
685 2012.
- 686 Hafner, B. D., Tomasella, M., Häberle, K.-H., Goebel, M., Matyssek, R., and Grams, T. E. E.: Hydraulic
687 redistribution under moderate drought among English oak, European beech and Norway spruce
688 determined by deuterium isotope labeling in a split-root experiment, *Tree Physiology*, 37, 950–960,
689 <https://doi.org/10.1093/treephys/tpx050>, 2017.
- 690 Hafner, B. D., Hesse, B. D., and Grams, T. E. E.: Friendly neighbours: Hydraulic redistribution accounts
691 for one quarter of water used by neighbouring drought stressed tree saplings, *Plant, Cell & Environment*,
692 44, 1243–1256, <https://doi.org/10.1111/pce.13852>, 2021.
- 693 Hildebrandt, A.: Root-Water Relations and Interactions in Mixed Forest Settings, in: *Forest-Water*
694 *Interactions*, edited by: Levia, D. F., Carlyle-Moses, D. E., Iida, S., Michalzik, B., Nanko, K., and Tischer,
695 A., Springer International Publishing, Cham, 319–348, https://doi.org/10.1007/978-3-030-26086-6_14,
696 2020.



- 697 Hildebrandt, A., Kleidon, A., and Bechmann, M.: A thermodynamic formulation of root water uptake,
698 *Hydrol. Earth Syst. Sci.*, 14, 2016.
- 699 Hopmans, J. W. and Bristow, K. L.: Current Capabilities and Future Needs of Root Water and Nutrient
700 Uptake Modeling, in: *Advances in Agronomy*, vol. 77, Elsevier, 103–183, [https://doi.org/10.1016/S0065-2113\(02\)77014-4](https://doi.org/10.1016/S0065-2113(02)77014-4), 2002.
- 702 Hupet, F. and Vanclooster, M.: Micro-variability of hydrological processes at the maize row scale:
703 implications for soil water content measurements and evapotranspiration estimates, *Journal of Hydrology*,
704 303, 247–270, <https://doi.org/10.1016/j.jhydrol.2004.07.017>, 2005.
- 705 Hupet, F., Lambot, S., Javaux, M., and Vanclooster, M.: On the identification of macroscopic root water
706 uptake parameters from soil water content observations, *Water Resources Research*, 38, 36-1-36-14,
707 <https://doi.org/10.1029/2002WR001556>, 2002.
- 708 IUSS Working Group, W. and others: World reference base for soil resources, *World Soil Resources*
709 Report, 103, 2006.
- 710 Ivanov, V. Y., Fatichi, S., Jenerette, G. D., Espeleta, J. F., Troch, P. A., and Huxman, T. E.: Hysteresis
711 of soil moisture spatial heterogeneity and the “homogenizing” effect of vegetation, *Water Resources*
712 *Research*, 46, <https://doi.org/10.1029/2009WR008611>, 2010.
- 713 Jackisch, C., Knoblauch, S., Blume, T., Zehe, E., and Hassler, S. K.: Estimates of tree root water uptake
714 from soil moisture profile dynamics, *Biogeosciences*, 17, 5787–5808, <https://doi.org/10.5194/bg-17-5787-2020>, 2020.
- 716 Jarecke, K. M., Bladon, K. D., and Wondzell, S. M.: The Influence of Local and Nonlocal Factors on Soil
717 Water Content in a Steep Forested Catchment, *Water Resources Research*, 57, e2020WR028343,
718 <https://doi.org/10.1029/2020WR028343>, 2021.
- 719 Jonard, F., André, F., Ponette, Q., Vincke, C., and Jonard, M.: Sap flux density and stomatal conductance
720 of European beech and common oak trees in pure and mixed stands during the summer drought of 2003,
721 *Journal of Hydrology*, 409, 371–381, <https://doi.org/10.1016/j.jhydrol.2011.08.032>, 2011.
- 722 Jost, G., Schume, H., and Hager, H.: Factors controlling soil water-recharge in a mixed European beech
723 (*Fagus sylvatica* L.)–Norway spruce [*Picea abies* (L.) Karst.] stand, *Eur J Forest Res*, 123, 93–104,
724 <https://doi.org/10.1007/s10342-004-0033-7>, 2004.
- 725 Katul, G. G. and Siqueira, M. B.: Biotic and abiotic factors act in coordination to amplify hydraulic
726 redistribution and lift, *The New Phytologist*, 187, 3–6, 2010.
- 727 Keim, R. F., Skaugset, A. E., and Weiler, M.: Temporal persistence of spatial patterns in throughfall,
728 *Journal of Hydrology*, 314, 263–274, <https://doi.org/10.1016/j.jhydrol.2005.03.021>, 2005.



- 729 Keim, R. F., Skaugset, A. E., and Weiler, M.: Storage of water on vegetation under simulated rainfall of
730 varying intensity, *Advances in Water Resources*, 29, 974–986,
731 <https://doi.org/10.1016/j.advwatres.2005.07.017>, 2006.
- 732 Kirchen, G., Calvaruso, C., Granier, A., Redon, P.-O., Van der Heijden, G., Bréda, N., and Turpault, M.-
733 P.: Local soil type variability controls the water budget and stand productivity in a beech forest, *Forest
734 Ecology and Management*, 390, 89–103, <https://doi.org/10.1016/j.foreco.2016.12.024>, 2017.
- 735 Kleidon, A. and Renner, M.: Thermodynamic limits of hydrologic cycling within the Earth system:
736 concepts, estimates and implications, *Hydrol. Earth Syst. Sci.*, 17, 2873–2892,
737 <https://doi.org/10.5194/hess-17-2873-2013>, 2013.
- 738 Klein, T., Rotenberg, E., Cohen-Hilaleh, E., Raz-Yaseef, N., Tatarinov, F., Preisler, Y., Ogée, J., Cohen,
739 S., and Yakir, D.: Quantifying transpirable soil water and its relations to tree water use dynamics in a
740 water-limited pine forest, *Ecohydrology*, 7, 409–419, <https://doi.org/10.1002/eco.1360>, 2014.
- 741 Kohlhepp, B., Lehmann, R., Seeber, P., Küsel, K., Trumbore, S. E., and Totsche, K. U.: Aquifer
742 configuration and geostructural links control the groundwater quality in thin-bedded carbonate–
743 siliciclastic alternations of the Hainich CZE, central Germany, *Hydrol. Earth Syst. Sci.*, 21, 6091–6116,
744 <https://doi.org/10.5194/hess-21-6091-2017>, 2017.
- 745 Krämer, I. and Hölscher, D.: Soil water dynamics along a tree diversity gradient in a deciduous forest in
746 Central Germany, *Ecohydrology*, 3, 262–271, <https://doi.org/10.1002/eco.103>, 2010.
- 747 Kreuzwieser, J. and Gessler, A.: Global climate change and tree nutrition: influence of water availability,
748 *Tree Physiology*, 30, 1221–1234, <https://doi.org/10.1093/treephys/tpq055>, 2010.
- 749 Kühnhammer, K., Kübert, A., Brüggemann, N., Deseano Diaz, P., van Dusschoten, D., Javaux, M., Merz,
750 S., Vereecken, H., Dubbert, M., and Rothfuss, Y.: Investigating the root plasticity response of *Centaurea
751 jacea* to soil water availability changes from isotopic analysis, *New Phytologist*, 226, 98–110,
752 <https://doi.org/10.1111/nph.16352>, 2020.
- 753 Kunert, N., Schwendenmann, L., Potvin, C., and Hölscher, D.: Tree diversity enhances tree transpiration
754 in a Panamanian forest plantation, *Journal of Applied Ecology*, 49, 135–144,
755 <https://doi.org/10.1111/j.1365-2664.2011.02065.x>, 2012.
- 756 Küsel, K., Totsche, K. U., Trumbore, S. E., Lehmann, R., Steinhäuser, C., and Herrmann, M.: How Deep
757 Can Surface Signals Be Traced in the Critical Zone? Merging Biodiversity with Biogeochemistry
758 Research in a Central German Muschelkalk Landscape, *Frontiers in Earth Science*, 4,
759 <https://doi.org/10.3389/feart.2016.00032>, 2016.
- 760 Lee, E., Kumar, P., Barron-Gafford, G. A., Hendryx, S. M., Sanchez-Cañete, E. P., Minor, R. L., Colella,
761 T., and Scott, R. L.: Impact of Hydraulic Redistribution on Multispecies Vegetation Water Use in a



- 762 Semiarid Savanna Ecosystem: An Experimental and Modeling Synthesis, *Water Resour. Res.*, 54, 4009–
763 4027, <https://doi.org/10.1029/2017WR021006>, 2018.
- 764 Leuschner, C.: Drought response of European beech (*Fagus sylvatica* L.)—A review, *Perspectives in*
765 *Plant Ecology, Evolution and Systematics*, 47, 125576, <https://doi.org/10.1016/j.ppees.2020.125576>,
766 2020.
- 767 Levia, D. F. and Frost, E. E.: A review and evaluation of stemflow literature in the hydrologic and
768 biogeochemical cycles of forested and agricultural ecosystems, *Journal of Hydrology*, 274, 1–29,
769 [https://doi.org/10.1016/S0022-1694\(02\)00399-2](https://doi.org/10.1016/S0022-1694(02)00399-2), 2003.
- 770 Levia, D. F. and Frost, E. E.: Variability of throughfall volume and solute inputs in wooded ecosystems,
771 *Progress in Physical Geography: Earth and Environment*, 30, 605–632,
772 <https://doi.org/10.1177/0309133306071145>, 2006.
- 773 Levia, D. F., Keim, R. F., Carlyle-Moses, D. E., and Frost, E. E.: Throughfall and Stemflow in Wooded
774 Ecosystems, in: *Forest Hydrology and Biogeochemistry: Synthesis of Past Research and Future*
775 *Directions*, edited by: Levia, D. F., Carlyle-Moses, D., and Tanaka, T., Springer Netherlands, Dordrecht,
776 425–443, https://doi.org/10.1007/978-94-007-1363-5_21, 2011.
- 777 Levia, D. F., Hudson, S. A., Llorens, P., and Nanko, K.: Throughfall drop size distributions: a review and
778 prospectus for future research: Throughfall drop size distributions, *WIREs Water*, 4, e1225,
779 <https://doi.org/10.1002/wat2.1225>, 2017.
- 780 Lhomme, J.-P.: Formulation of root water uptake in a multi-layer soil-plant model: does van den Honert’s
781 equation hold?, *Hydrology and Earth System Sciences*, 2, 31–39, <https://doi.org/10.5194/hess-2-31-1998>,
782 1998.
- 783 Looy, K. V., Bouma, J., Herbst, M., Koestel, J., Minasny, B., Mishra, U., Montzka, C., Nemes, A.,
784 Pachepsky, Y. A., Padarian, J., Schaap, M. G., Tóth, B., Verhoef, A., Vanderborght, J., Ploeg, M. J. van
785 der, Weihermüller, L., Zacharias, S., Zhang, Y., and Vereecken, H.: Pedotransfer Functions in Earth
786 System Science: Challenges and Perspectives, *Reviews of Geophysics*, 55, 1199–1256,
787 <https://doi.org/10.1002/2017RG000581>, 2017.
- 788 Lübbe, T., Schuldt, B., Coners, H., and Leuschner, C.: Species diversity and identity effects on the water
789 consumption of tree sapling assemblages under ample and limited water supply, *Oikos*, 125, 86–97,
790 <https://doi.org/10.1111/oik.02367>, 2016.
- 791 Lüdecke, D., Ben-Shachar, M., Patil, I., Waggoner, P., and Makowski, D.: performance: An R Package
792 for Assessment, Comparison and Testing of Statistical Models, *JOSS*, 6, 3139,
793 <https://doi.org/10.21105/joss.03139>, 2021.



- 794 Magh, R.-K., Eiferle, C., Burzlaff, T., Dannenmann, M., Rennenberg, H., and Dubbert, M.: Competition
795 for water rather than facilitation in mixed beech-fir forests after drying-wetting cycle, *Journal of*
796 *Hydrology*, 587, 124944, <https://doi.org/10.1016/j.jhydrol.2020.124944>, 2020.
- 797 Magliano, P. N., Whitworth-Hulse, J. I., Florio, E. L., Aguirre, E. C., and Blanco, L. J.: Interception loss,
798 throughfall and stemflow by *Larrea divaricata*: The role of rainfall characteristics and plant morphological
799 attributes, *Ecological Research*, 34, 753–764, <https://doi.org/10.1111/1440-1703.12036>, 2019.
- 800 Martínez García, G., Pachepsky, Y. A., and Vereecken, H.: Effect of soil hydraulic properties on the
801 relationship between the spatial mean and variability of soil moisture, *Journal of Hydrology*, 516, 154–
802 160, <https://doi.org/10.1016/j.jhydrol.2014.01.069>, 2014.
- 803 Meißner, M., Köhler, M., Schwendenmann, L., and Hölscher, D.: Partitioning of soil water among canopy
804 trees during a soil desiccation period in a temperate mixed forest, *Biogeosciences*, 9, 3465–3474,
805 <https://doi.org/10.5194/bg-9-3465-2012>, 2012.
- 806 Metzger, J. C., Wutzler, T., Valle, N. D., Filipzik, J., Grauer, C., Lehmann, R., Roggenbuck, M.,
807 Schelhorn, D., Weckmüller, J., Küsel, K., Totsche, K. U., Trumbore, S., and Hildebrandt, A.: Vegetation
808 impacts soil water content patterns by shaping canopy water fluxes and soil properties, *Hydrological*
809 *Processes*, 31, 3783–3795, <https://doi.org/10.1002/hyp.11274>, 2017.
- 810 Metzger, J. C., Filipzik, J., Michalzik, B., and Hildebrandt, A.: Stemflow Infiltration Hotspots Create Soil
811 Microsites Near Tree Stems in an Unmanaged Mixed Beech Forest, *Front. For. Glob. Change*, 4, 701293,
812 <https://doi.org/10.3389/ffgc.2021.701293>, 2021.
- 813 Molina, A. J., Llorens, P., Garcia-Estringana, P., Moreno de las Heras, M., Cayuela, C., Gallart, F., and
814 Latron, J.: Contributions of throughfall, forest and soil characteristics to near-surface soil water-content
815 variability at the plot scale in a mountainous Mediterranean area, *Science of The Total Environment*, 647,
816 1421–1432, <https://doi.org/10.1016/j.scitotenv.2018.08.020>, 2019.
- 817 Nadezhdina, N., Cermak, J., Meiresonne, L., and Ceulemans, R.: Transpiration of Scots pine in Flanders
818 growing on soil with irregular substratum, *Forest Ecology and Management*, 9, 2007.
- 819 Neumann, R. B. and Cardon, Z. G.: The magnitude of hydraulic redistribution by plant roots: a review
820 and synthesis of empirical and modeling studies, *New Phytologist*, 194, 337–352,
821 <https://doi.org/10.1111/j.1469-8137.2012.04088.x>, 2012.
- 822 Nie, C., Huang, Y., Zhang, S., Yang, Y., Zhou, S., Lin, C., and Wang, G.: Effects of soil water content
823 on forest ecosystem water use efficiency through changes in transpiration/evapotranspiration ratio,
824 *Agricultural and Forest Meteorology*, 308–309, 108605,
825 <https://doi.org/10.1016/j.agrformet.2021.108605>, 2021.



- 826 Obladen, N., Dechering, P., Skiadaresis, G., Tegel, W., Keßler, J., Höllerl, S., Kaps, S., Hertel, M.,
827 Dulamsuren, C., Seifert, T., Hirsch, M., and Seim, A.: Tree mortality of European beech and Norway
828 spruce induced by 2018–2019 hot droughts in central Germany, *Agricultural and Forest Meteorology*,
829 307, 108482, <https://doi.org/10.1016/j.agrformet.2021.108482>, 2021.
- 830 Otto, J., Berveiller, D., Bréon, F.-M., Delpierre, N., Geppert, G., Granier, A., Jans, W., Knohl, A., Kuusk,
831 A., Longdoz, B., Moors, E., Mund, M., Pinty, B., Schelhaas, M.-J., and Luysaert, S.: Forest summer
832 albedo is sensitive to species and thinning: how should we account for this in Earth system models?,
833 *Biogeosciences*, 11, 2411–2427, <https://doi.org/10.5194/bg-11-2411-2014>, 2014.
- 834 Pearson, R. K.: Data cleaning for dynamic modeling and control, in: 1999 European Control Conference
835 (ECC), 1999 European Control Conference (ECC), 2584–2589,
836 <https://doi.org/10.23919/ECC.1999.7099714>, 1999.
- 837 Pretzsch, H., Schütze, G., and Uhl, E.: Resistance of European tree species to drought stress in mixed
838 versus pure forests: evidence of stress release by inter-specific facilitation, *Plant Biology*, 15, 483–495,
839 <https://doi.org/10.1111/j.1438-8677.2012.00670.x>, 2013.
- 840 Priyadarshini, K. V. R., Prins, H. H. T., de Bie, S., Heitkönig, I. M. A., Woodborne, S., Gort, G., Kirkman,
841 K., Ludwig, F., Dawson, T. E., and de Kroon, H.: Seasonality of hydraulic redistribution by trees to
842 grasses and changes in their water-source use that change tree-grass interactions: HYDRAULIC
843 REDISTRIBUTION BY TREES TO GRASSES AND CHANGES IN THEIR WATER SOURCES,
844 *Ecohydrol.*, 9, 218–228, <https://doi.org/10.1002/eco.1624>, 2016.
- 845 Pypker, T. G., Levia, D. F., Staelens, J., and Van Stan, J. T.: Canopy Structure in Relation to Hydrological
846 and Biogeochemical Fluxes, in: *Forest Hydrology and Biogeochemistry: Synthesis of Past Research and
847 Future Directions*, edited by: Levia, D. F., Carlyle-Moses, D., and Tanaka, T., Springer Netherlands,
848 Dordrecht, 371–388, https://doi.org/10.1007/978-94-007-1363-5_18, 2011.
- 849 R Core Team: R: The R Project for Statistical Computing, R Foundation for Statistical Computing,
850 Vienna, Austria, 2021.
- 851 Raat, K. J., Draaijers, G. P. J., Schaap, M. G., Tietema, A., and Verstraten, J. M.: Spatial variability of
852 throughfall water and chemistry and forest floor water content in a Douglas fir forest stand, *Hydrol. Earth
853 Syst. Sci.*, 6, 363–374, <https://doi.org/10.5194/hess-6-363-2002>, 2002.
- 854 del Río, M., Schütze, G., and Pretzsch, H.: Temporal variation of competition and facilitation in mixed
855 species forests in Central Europe, *Plant Biology*, 16, 166–176, <https://doi.org/10.1111/plb.12029>, 2014.
- 856 Rodrigues, A. F., Terra, M. C. N. S., Mantovani, V. A., Cordeiro, N. G., Ribeiro, J. P. C., Guo, L., Nehren,
857 U., Mello, J. M., and Mello, C. R.: Throughfall spatial variability in a neotropical forest: Have we
858 correctly accounted for time stability?, *Journal of Hydrology*, 608, 127632,
859 <https://doi.org/10.1016/j.jhydrol.2022.127632>, 2022.



- 860 Rodríguez-Robles, U., Arredondo, J. T., Huber-Sannwald, E., Yépez, E. A., and Ramos-Leal, J. A.:
861 Coupled plant traits adapted to wetting/drying cycles of substrates co-define niche multidimensionality,
862 *Plant, Cell & Environment*, 43, 2394–2408, <https://doi.org/10.1111/pce.13837>, 2020.
- 863 Rosenbaum, U., Bogena, H. R., Herbst, M., Huisman, J. A., Peterson, T. J., Weuthen, A., Western, A.
864 W., and Vereecken, H.: Seasonal and event dynamics of spatial soil moisture patterns at the small
865 catchment scale: DYNAMICS OF CATCHMENT-SCALE SOIL MOISTURE PATTERNS, *Water*
866 *Resour. Res.*, 48, <https://doi.org/10.1029/2011WR011518>, 2012.
- 867 Sadeghi, S. M. M., Gordon, D. A., and Van Stan II, J. T.: A Global Synthesis of Throughfall and Stemflow
868 Hydrometeorology, in: *Precipitation Partitioning by Vegetation: A Global Synthesis*, edited by: Van Stan,
869 I., John T., Gutmann, E., and Friesen, J., Springer International Publishing, Cham, 49–70,
870 https://doi.org/10.1007/978-3-030-29702-2_4, 2020.
- 871 Schume, H., Jost, G., and Hager, H.: Soil water depletion and recharge patterns in mixed and pure forest
872 stands of European beech and Norway spruce, *Journal of Hydrology*, 289, 258–274,
873 <https://doi.org/10.1016/j.jhydrol.2003.11.036>, 2004.
- 874 Schwärzel, K., Menzer, A., Clausnitzer, F., Spank, U., Häntzschel, J., Grünwald, T., Köstner, B.,
875 Bernhofer, C., and Feger, K.-H.: Soil water content measurements deliver reliable estimates of water
876 fluxes: A comparative study in a beech and a spruce stand in the Tharandt forest (Saxony, Germany),
877 *Agricultural and Forest Meteorology*, 149, 1994–2006, <https://doi.org/10.1016/j.agrformet.2009.07.006>,
878 2009.
- 879 Seeger, S. and Weiler, M.: Temporal dynamics of tree xylem water isotopes: in situ monitoring and
880 modeling, *Biogeosciences*, 18, 4603–4627, <https://doi.org/10.5194/bg-18-4603-2021>, 2021.
- 881 Shachnovich, Y., Berliner, P. R., and Bar, P.: Rainfall interception and spatial distribution of throughfall
882 in a pine forest planted in an arid zone, *Journal of Hydrology*, 349, 168–177,
883 <https://doi.org/10.1016/j.jhydrol.2007.10.051>, 2008.
- 884 Shani, U. and Dudley, L. M.: Modeling water uptake by roots under water and salt stress: Soil-based and
885 crop response root sink terms, *Plant Roots: The Hidden Half*, 635–641, 1996.
- 886 Silvertown, J., Araya, Y., and Gowing, D.: Hydrological niches in terrestrial plant communities: a review,
887 *Journal of Ecology*, 103, 93–108, <https://doi.org/10.1111/1365-2745.12332>, 2015.
- 888 Spanner, G. C., Gimenez, B. O., Wright, C. L., Menezes, V. S., Newman, B. D., Collins, A. D., Jardine,
889 K. J., Negrón-Juárez, R. I., Lima, A. J. N., Rodrigues, J. R., Chambers, J. Q., Higuchi, N., and Warren, J.
890 M.: Dry Season Transpiration and Soil Water Dynamics in the Central Amazon, *Frontiers in Plant*
891 *Science*, 13, 2022.



- 892 Staelens, J., De Schrijver, A., Verheyen, K., and Verhoest, N. E. C.: Spatial variability and temporal
893 stability of throughfall water under a dominant beech (*Fagus sylvatica* L.) tree in relationship to canopy
894 cover, *Journal of Hydrology*, 330, 651–662, <https://doi.org/10.1016/j.jhydrol.2006.04.032>, 2006.
- 895 Staelens, J., De Schrijver, A., Verheyen, K., and Verhoest, N. E. C.: Rainfall partitioning into throughfall,
896 stemflow, and interception within a single beech (*Fagus sylvatica* L.) canopy: influence of foliation, rain
897 event characteristics, and meteorology, *Hydrological Processes*, 22, 33–45,
898 <https://doi.org/10.1002/hyp.6610>, 2008.
- 899 Teuling, A. J. and Troch, P. A.: Improved understanding of soil moisture variability dynamics,
900 *Geophysical Research Letters*, 32, <https://doi.org/10.1029/2004GL021935>, 2005.
- 901 Thieurmél, B. and Elmarhraoui, A.: suncalc: Compute Sun Position, Sunlight Phases, Moon Position and
902 Lunar Phase, 2022.
- 903 Vachaud, G., Passerat De Silans, A., Balabanis, P., and Vauclin, M.: Temporal Stability of Spatially
904 Measured Soil Water Probability Density Function, *Soil Science Society of America Journal*, 49, 822–
905 828, <https://doi.org/10.2136/sssaj1985.03615995004900040006x>, 1985.
- 906 Van Stan, J. T., Siegert, C. M., Levia, D. F., and Scheick, C. E.: Effects of wind-driven rainfall on
907 stemflow generation between codominant tree species with differing crown characteristics, *Agricultural
908 and Forest Meteorology*, 151, 1277–1286, <https://doi.org/10.1016/j.agrformet.2011.05.008>, 2011.
- 909 Van Stan, J. T., Hildebrandt, A., Friesen, J., Metzger, J. C., and Yankine, S. A.: Spatial Variability and
910 Temporal Stability of Local Net Precipitation Patterns, in: *Precipitation Partitioning by Vegetation: A
911 Global Synthesis*, edited by: Van Stan, I., John T., Gutmann, E., and Friesen, J., Springer International
912 Publishing, Cham, 89–104, https://doi.org/10.1007/978-3-030-29702-2_6, 2020.
- 913 Vereecken, H., Kamai, T., Harter, T., Kasteel, R., Hopmans, J., and Vanderborght, J.: Explaining soil
914 moisture variability as a function of mean soil moisture: A stochastic unsaturated flow perspective,
915 *Geophysical Research Letters*, 34, <https://doi.org/10.1029/2007GL031813>, 2007.
- 916 Vereecken, H., Amelung, W., Bauke, S. L., Bogaen, H., Brüggemann, N., Montzka, C., Vanderborght,
917 J., Bechtold, M., Blöschl, G., Carminati, A., Javaux, M., Konings, A. G., Kusche, J., Neuweiler, I., Or,
918 D., Steele-Dunne, S., Verhoef, A., Young, M., and Zhang, Y.: Soil hydrology in the Earth system, *Nat
919 Rev Earth Environ*, 3, 573–587, <https://doi.org/10.1038/s43017-022-00324-6>, 2022.
- 920 Vitali, V., Forrester, D. I., and Bauhus, J.: Know Your Neighbours: Drought Response of Norway Spruce,
921 Silver Fir and Douglas Fir in Mixed Forests Depends on Species Identity and Diversity of Tree
922 Neighbourhoods, *Ecosystems*, 21, 1215–1229, <https://doi.org/10.1007/s10021-017-0214-0>, 2018.



- 923 Volkmann, T. H. M., Haberer, K., Gessler, A., and Weiler, M.: High-resolution isotope measurements
924 resolve rapid ecohydrological dynamics at the soil–plant interface, *New Phytologist*, 210, 839–849,
925 <https://doi.org/10.1111/nph.13868>, 2016.
- 926 Wambsganss, J., Beyer, F., Freschet, G. T., Scherer-Lorenzen, M., and Bauhus, J.: Tree species mixing
927 reduces biomass but increases length of absorptive fine roots in European forests, *J Ecol*, 109, 2678–
928 2691, <https://doi.org/10.1111/1365-2745.13675>, 2021.
- 929 Whelan, M. J. and Anderson, J. M.: Modelling spatial patterns of throughfaU and interception loss in a
930 Norway spruce (*Picea abies*) plantation at the plot scale, *Journal of Hydrology*, 186, 335–354, 1996.
- 931 Wiekenkamp, I., Huisman, J. A., Bogena, H. R., Lin, H. S., and Vereecken, H.: Spatial and temporal
932 occurrence of preferential flow in a forested headwater catchment, *Journal of Hydrology*, 534, 139–149,
933 <https://doi.org/10.1016/j.jhydrol.2015.12.050>, 2016.
- 934 Wullaert, H., Pohlert, T., Boy, J., Valarezo, C., and Wilcke, W.: Spatial throughfall heterogeneity in a
935 montane rain forest in Ecuador: Extent, temporal stability and drivers, *Journal of Hydrology*, 377, 71–79,
936 <https://doi.org/10.1016/j.jhydrol.2009.08.001>, 2009.
- 937 Yu, K. and D’Odorico, P.: Hydraulic lift as a determinant of tree–grass coexistence on savannas, *New*
938 *Phytologist*, 207, 1038–1051, <https://doi.org/10.1111/nph.13431>, 2015.
- 939 Zacharias, S. and Wessolek, G.: Excluding Organic Matter Content from Pedotransfer Predictors of Soil
940 Water Retention, *Soil Science Society of America Journal*, 71, 43–50,
941 <https://doi.org/10.2136/sssaj2006.0098>, 2007.
- 942 Zehe, E., Graeff, T., Morgner, M., Bauer, A., and Bronstert, A.: Plot and field scale soil moisture
943 dynamics and subsurface wetness control on runoff generation in a headwater in the Ore Mountains,
944 *Hydrol. Earth Syst. Sci.*, 14, 873–889, <https://doi.org/10.5194/hess-14-873-2010>, 2010.
- 945 Zhang, Y., Wang, X., Hu, R., and Pan, Y.: Throughfall and its spatial variability beneath xerophytic shrub
946 canopies within water-limited arid desert ecosystems, *Journal of Hydrology*, 539, 406–416,
947 <https://doi.org/10.1016/j.jhydrol.2016.05.051>, 2016.
- 948 Zhu, X., He, Z., Du, J., Chen, L., Lin, P., and Tian, Q.: Spatial heterogeneity of throughfall and its
949 contributions to the variability in near-surface soil water-content in semiarid mountains of China, *Forest*
950 *Ecology and Management*, 488, 119008, <https://doi.org/10.1016/j.foreco.2021.119008>, 2021.
- 951 Zimmermann, A., Zimmermann, B., and Elsenbeer, H.: Rainfall redistribution in a tropical forest: Spatial
952 and temporal patterns, *Water Resour. Res.*, 45, <https://doi.org/10.1029/2008WR007470>, 2009.



953 Zuur, A. F., Ieno, E. N., Walker, N., Saveliev, A. A., and Smith, G. M.: Mixed effects models and
954 extensions in ecology with R, Springer New York, New York, NY, [https://doi.org/10.1007/978-0-387-](https://doi.org/10.1007/978-0-387-87458-6)
955 87458-6, 2009.

956